LI DISTRIBUTION BETWEEN CHLORITE

AND ALBITE IN A COMMON VAPOR PHASE

By

Ⓒ

PETER VILKS, B.SC.

A Thesis

Submitted to the School of Graduate Studies

in Partial Fulfilment of the Requirements

for the Degree

Master of Science

McMaster University

March 1981

MASTER OF SCIENCE (1981)　　　　　　　　　McMASTER UNIVERSITY

(Geology)　　　　　　　　　　　　　　　　　Hamilton, Ontario

TITLE:　　Li Distribution between Chlorite and Albite in

a Common Vapor Phase

AUTHOR:　Peter Vilks, B.Sc.　　(Dalhousie University)

SUPERVISOR:　Denis M. Shaw

NUMBER OF PAGES:　i-x, 1-95

ii

ABSTRACT

This study attempted to examine the process of Li enrichment in spilites by testing the hypothesis that Li is concentrated in metamorphosed basalts from hydrothermal solutions in the temperature range 400^0 to 700^0 C and at a 1.5 kb pressure. Using a double-capsule technique Li was partitioned between albite and chlorite in a common vapor phase. These minerals were used since they are commonly found in the greenschist facies and chlorite is suspected to be the main Li host. The chlorite (clinochlore) and albite were grown from synthetic gels. A few experiments were also attempted with a natural albite and natural Fe-chlorite. Li analysis was carried out by atomic absorption and neutron activation.

A variation between temperature and the partition coefficient of Li between albite and chlorite could not be resolved. Therefore, the average partition coefficient from all synthetic experiments was $D^{alb-chl} = 0.56 \pm .06$. The partition coefficient in the natural system was not significantly higher ($D^{alb-chl} = 0.81 \pm .46$). Considerable doubt exists as to the accuracy of the vapor-mineral partition coefficients because of the poor Li mass balance. A range of possible vapor-mineral distributions was obtained:

	measured	predicted from Li mass balance
$D^{vap-alb}$	2.77 ± 6.45	5.97 ± 7.99
$D^{vap-chl}$	1.10 ± 2.31	2.89 ± 3.34

The measured Li partition coefficients do not explain the behavior of Li in spilites because too much Li went into the albite, and the $D^{vap-chl}$ was not less than 1.00 so that most hydrothermal waters do not contain enough Li to produce the observed enrichment in spilites. Lithium may be precipitated in spilites at lower temperatures or pressures than those in this study.

ACKNOWLEDGEMENTS

TABLE OF CONTENTS

LIST OF TABLES

LIST OF FIGURES

x

INTRODUCTION

I-1 Purpose of the study

Shaw et. al. (1977) have shown that spilitised basalts contain more Li (average = 75 ppm) than fresh basalts (average = 12 ppm). Lithium was shown to increase with weight percent H_2O and with a decrease in the ratio CaO/Al_2O_3. Since H_2O increases and CaO decreases with spilitisation of basalts Shaw et. al. (1977) suggest that Li increase is characteristic of spilitization.

Shaw et. al. (1977) predicted the Li/Na ratio of the fluids which produce spilitisation. These predictions were limited because the mechanism of Li uptake in spilites is not clearly understood. Floyd (1977) indicated that Li was enriched in chlorite-rich patches. Unpublished ion probe data of J. V. Smith also show that Li is concentrated in chlorite.

The purpose of this study is to improve our understanding of Li behavior during spilitisation. Two essential secondary minerals in spilites are chlorite and albite. Therefore, this study will try to determine the distribution of Li between these two minerals in a common vapor phase. This would demonstrate whether or not Li prefers to enter chlorite. The Li/Na ratio of the hydrothermal fluid and the effect of temperature will also be studied.

1

In summary, this study will test the hypothesis that Li distribution between albite and chlorite in a common vapor phase at 400 to 700^0 C and 1.5 kb can explain Li uptake in spilitised basalts.

I-2 Previous work on Li distribution

Volfinger (1970) measured Li and K exchange between muscovite and vapor, and sanidine and vapor at 600^0 C and 1 kb. Muscovite might be considered as a mica analogue to chlorite, and sanidine as an analogue to albite. The exchange isotherms for both minerals are curved with the increasing atomic ratio of Li/K (Figures I-1 and I-2). Lithium prefers to enter muscovite between a $\log_{10}$ (Li/K)$_{musc}$ of -2.5 and -1. Volfinger and Robert (1979) measured Li and K exchange between phlogopite and vapor (Figure I-3). This exchange isotherm is also curved with Li prefering to enter phlogopite at $\log_{10}$ (Li/K)$_{phlog}$ less than -2.3.

Matsui et. al. (1977) reported partition coefficients between phenocrysts and groundmass for Li and other elements. The minerals included olivine, augite, plagioclase ($D_{Li}^{groundmass-min}$ = 0.20), hornblende and biotite. A plagioclase/augite Li distribution in a bronzitite was $D_{Li}^{plag-aug}$ = 0.76. The authors also used Onuma diagrams to show that Li should enter the same sites as Mg.

Liotard et. al. (1979) measured partition coefficients between plagioclase and matrix from a calk-alkaline suite in Peru. In andesite $D_{Li}^{matrix-plag}$ varied from 0.40 to 2.27. In dacite $D_{Li}^{matrix-plag}$ was 0.56 to 4.17. In rhyolite $D_{Li}^{matrix-plag}$ was 0.25 to 0.36.

Figure I-1 Li/K exchange isotherms between sanidine and mus-

covite and a vapor phase at 600^0 C and 1 kb. Ratios are in atomic

numbers. (Volfinger, 1970)·

Figure I-2 Li/K exchange isotherm between sanidine and muscovite

at 600^0 C and 1 kb. The isotherm is calculated from the results

in figure I-1. (Volfinger, 1970)

Figure I-3 Li/K exchange isotherm between vapor and phlogopite

at 600^0 C and 1 kb. Ratios are in atomic numbers. (Volfinger

and Robert, 1979)

3
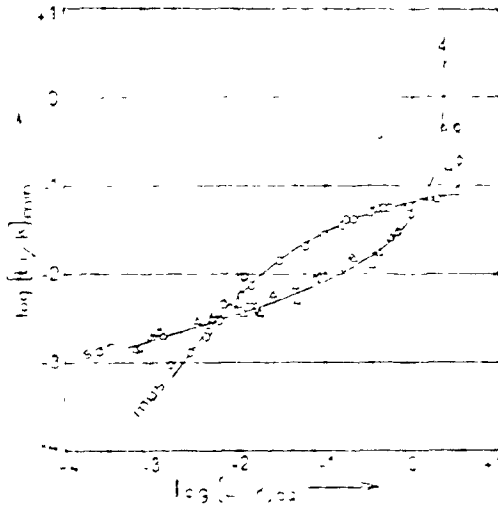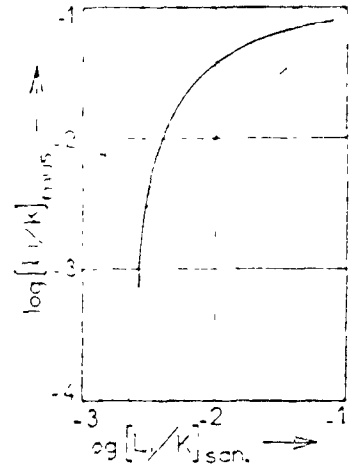
Figure I-1

Figure I-2
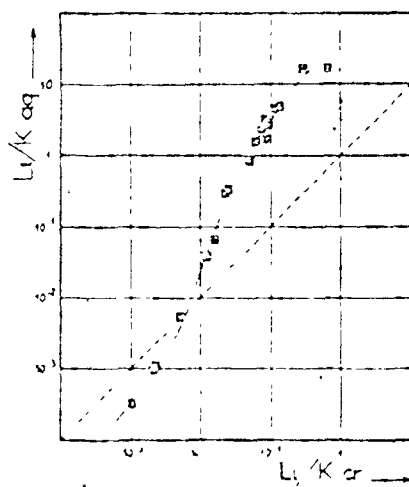
Figure I-3

I-3 Geochemistry of lithium

Lithium is a group 1 alkali metal with the atomic number of 3 and an atomic weight of 6.94. It has two naturally occurring isotopes (^6Li = 7.4%; ^7Li = 92.6%).

Lithium has two electrons in the s-1 orbital and one electron in the s-2 orbital. The latter electron is lost very easily, leaving it with the electron configuration of helium. Since Li is easily ionized into a cation it is very reactive. Lithium has the highest polarizing power of all the alkalies. This leads to low solubilities of various salts such as the fluoride, carbonate, and phosphate, and to a tendancy for covalent bond formation and solvation.

The small size of the Li ion makes substitution with Na difficult. A similar ionic radius to Al^{+3}, Fe^{+2}, and Mg^{+2} makes substitution with these elements possible. Lithium has similar geochemical behaviour to Mg. In bonds with oxygen Li is found in four-fold and six-fold coordination. Other properties of Li, as well as Na, K, Rb, Cs, and Mg are summarized in table I-1.

In an exchange reaction with an anionic ligand the order of preference is Li < Na < K < Rb < Cs. If bonding is purely electrostatic the cation with the smallest solvation radius will be preferred. Lithium, with the largest solvation radius, is least preferred. (Cotton and Wilkinson).

Economic concentrations of Li may be recovered from certain pegmatites. Important Li minerals recovered from pegmatites include

spodumene ($LiAlSi_2O_6$), lepidolite ($K(Li,Al)_3(Si,Al)_4O_{10}(F,OH)_2$),
petalite ($LiAlSi_4O_{10}$), and the phosphate, amblygonite ($(Li,Na)Al(PO_4)$
(F,OH)). Li is also found concentrated in some hot springs and geysers.
At Clayton Valley, near Silver Peak, Nevada, Li is recovered from
brines containing an average of 300 ppm Li. In playas Li is concentrated
by evaporation along with other salts. In the sedimentary enviroment
Li may be concentrated in certain clay minerals (hectorite), manganese
oxides (lithiophorite), and phosphates (amblygonite, lithiophilite,
triphylite).

Table I-1 (Cotton and Wilkinson)

	Li	Na	K	Rb	Cs	Mg
ionization potential 1st	5.390	5.138	4.339	4.176	3.893	
ionization potential 2nd	75.62	47.29	31.81	27.36	23.4	
melting point ^{o}C	180.5	97.8	63.7	38.98	28.59	
boiling point ^{o}C	1326	883	756	688	690	
E^o (v) $(M^+_{aq} + e = M_s)$	-3.02	-2.71	-2.92	-2.99	-3.02	
Goldschmidt ionic r Å	0.78	0.98	1.33	1.49	1.65	0.78
Pauling ionic r Å	0.60	0.95	1.33	1.48	1.69	0.65
hydrated radius Å	3.40	2.76	2.32	2.28	2.28	

There is an increasing number of uses for Li (Vine,1976).
Thermonuclear power plants require tritium which can be produced by
bombarding Li with neutrons. Lithium will be needed for lightweight
batteries used in electric cars. Lithium bromide is useful in refri-
geration units because of its low vapor pressure. Other uses for
lithium include heat resistant glass and ceramics (Corning Ware),

special heat and water resistant lubricants, aluminum refining, cosmetics, paints and air purifying in submarines.

Heier and Billings (1970) give a very good summary of the geochemistry of lithium.

I-4 Definitions

If chlorite and albite are in equilibrium with the same vapor phase at constant temperature and pressure then the chemical potential of Li should be the same in both minerals and the vapor. The Li partitioning between albite and chlorite could be written as:

Li-chlorite + albite = Li-albite + chlorite
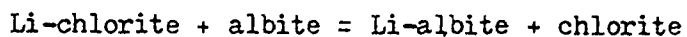
The equilibrium constant $(K^{alb-chl})$ for this reaction could be written as:

*

$$K^{alb-chl} = \frac{[\text{Li-albite}]\ [\text{chlorite}]}{[\text{Li-chlorite}]\ [\text{albite}]}$$

At infinite dilution of Li the activities of albite and chlorite approach unity so that $K^{alb-chl}$ becomes:

$$K^{alb-chl} = \frac{[\text{Li-albite}]}{[\text{Li-chlorite}]} = \frac{f^{alb}_{\text{Li-albite}}}{f^{chl}_{\text{Li-chlorite}}} \cdot \frac{X^{alb}_{\text{Li-albite}}}{X^{chl}_{\text{Li-chlorite}}}$$

[ ] = activity

$X^{chl}_{\text{Li-chlorite}}$ = mole fraction of Li-chlorite in chlorite

$f^{chl}_{\text{Li-chlorite}}$ = activity coefficient of Li-chlorite in chlorite

The distribution coefficient $(D^{alb-chl})$ is written as:

$$D^{alb-chl} = \frac{X^{alb}_{\text{Li-albite}}}{X^{chl}_{\text{Li-chlorite}}}$$

---

* This equilibrium constant is poorly defined because the exact mechanism of Li exchange is not known.

The distribution coefficient, $D^{alb-chl}$, will equal the equilibrium constant, $K^{alb-chl}$, only if the activity coefficients of Li in the two minerals are the same. When making calculations with trace elements it is often more convenient to deal with parts per million than with mole fractions. Therefore the distribution coefficients will be expressed as:

$$D^{alb-chl} = \frac{C_{Li}^{alb}}{C_{Li}^{chl}}$$

where: C_{Li}^{alb} = concentration of Li in albite in ppm

The distribution of Li between a mineral and the vapor phase can be expressed in a similar way. For example:

$$D^{vap-chl} = \frac{C_{Li}^{vap}}{C_{Li}^{chl}}$$

Note that:

$$D^{alb-chl} = \frac{D^{vap-chl}}{D^{vap-alb}}$$

An alternate way to express Li distribution is based on the assumption that Li exchanges with another element. Since Li is assumed to compete for the same site as Mg in chlorite, one could write the following reaction:

$$2Li\text{-chlorite} + Mg^{++} = Mg\text{-chlorite} + 2Li^{+}$$
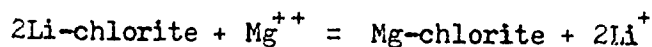
Then the Li-Mg exchange distribution coefficient is written as:

$$K_D^{vap-chl} = \frac{(C_{Li}^{vap})^2}{C_{Mg}^{vap}} \times \frac{C_{Mg}^{chl}}{(C_{Li}^{chl})^2}$$

Volfinger (1970), and Volfinger and Robert (1979) use a
similar formulation to describe Li and K exchange in muscovite, sanidine
and phlogopite. O'Nions and Powell (1977) describe some of the advan-
tages and disadvantages of D^{A-B} or K_D^{A-B} distribution coefficients.
When elemental ratios are used the distribution coefficient will be
less temperature and pressure sensitive because the changes in enthalpy,
and molar volume are smaller for such reactions. Element ratios would
also be less sensitive to changes in the composition of the vapor or
minerals. With increasing ionic strength activity coefficients in
the vapor will deviate from unity. The activity coefficients of the
two competing elements will change in a similar manner, particularlly
if they have the same charge. This would reduce the effect of ionic
strength on the distribution coefficient. If ligands are present in
solution, both elements might be complexed to the same degree, cancelling
the effect of the ligand. If both elements compete for the same sites
in the mineral (in similar proportions) then the concentration of
one element may affect the amount of the other element which is accepted
by the mineral.

The K_D type of distribution is not very convenient for
this study. The only major cations which albite and chlorite have in
common are Al^{+++} and Si^{+4}. Li is not expected to substitute for either
of these. Since Li has a close geochemical behavior to Mg, this element
should be an ideal choice for an exchange reaction with chlorite and
vapor. However, since Mg has a double charge, its activity coefficient
would vary with increasing ionic strength to a different degree than

that of Li (Garrels and Christ, 1965). Volfinger and Robert (1979) found no covariation between Mg and Li in a vapor phase which was in equilibrium with phlogopite. Therefore, the partition coefficients measured in this study will be the D type.

A convenient way to show the variation of partition coefficients with composition is by means of a distribution plot or a Roozeboom plot (Figures III-1 to 6). The concentration of an element in one phase is plotted against concentration in another phase. If the two phases were in equilibrium the distribution plot should give a line running through the origin. If the line does not run through the origin then equilibrium may not have been achieved, one phase may have been biased by a non-random analytical error, or crystal defects may have influenced the element's distribution. As long as the distribution coefficient (D) remains constant the Roozeboom plot will give a straight line. Any change in slope will mark the element concentration at which D begins to change with composition. Each linear portion of a Roozeboom plot can be described by a linear equation:

$$C_{Li}^{alb} = a_0 + a_1 C_{Li}^{chl}$$

The slope is given by a_1 and the intercept is a_0. The distribution coefficient for this portion of the curve is given by:

$$D^{alb-chl} = a_1 + a_0/C_{Li}^{chl}$$

A trace element's D value remains independent of its own abundance as long as the activity coefficients do not change (Henry's law is obeyed). Above a certain concentration the element's activity coefficient (f_i) will begin to change, making it difficult to relate

concentration (X_i) to activity. Mysen (1978) discusses limits of trace
element concentration which obey Henry's law. If a trace element subs-
titutes for a major element then the concentration limit of Henry's law
may depend on the difference between the two elements' ionic radii.
Iiyama and Volfinger (1976) have constructed a model which attempts to
explain deviations from Henry's law with increasing concentration. As
a trace element is taken in by a mineral the crystal is locally deformed,
limiting further intake of the trace element.

Most distribution coefficient theory is based on the assum-
ption that trace elements enter crystallographic sites. Plots of
partition coefficient versus ionic radius tend to support the view that
elements enter sites which prefer certain ionic sizes (Matsui et. al.,
1977). Crystal defects may also be an important location for trace
elements. Buseck and Veblen (1978) have used high resolution electron
microscopy to illustrate crystal defects. They point out that incom-
patible elements may be influenced by dislocation densities, particularly
if the amount of trace element is small. Compatible elements are not
greatly affected. Navrotsky (1978) also reviews the effect of defects
on trace element distributions. Along with temperature, pressure and
composition the number of defects may be influenced by the growth rate.
Multidimensional defects may remain as artifacts in real crystals
from growth, deformation, and temperature gradients.

I-5 Measurement of distribution coefficients

One approach to measuring partition coefficients is the analysis of minerals in natural rocks. For most major and minor elements the microprobe can be·used, while trace elements can be analysed by atomic absorption after mineral separation. The advantage of looking at natural minerals is that the measured distribution represents a real system. The disadvantages include poor control over the temperature and pressure of equilibration, little information on any vapor phase, and difficulties in mineral separation. Chlorite can be particularly difficult to separate because of its fine grain size.

Several techniques have been used experimentally to determine partition coefficients. Minerals have been grown from gels in equilibrium with a vapor phase (Volfinger (1970), Lagache (1971), and others). The mineral and solution are easily separated for analysis. Combined vapor-mineral distributions give mineral-mineral distributions. Several minerals have been equilibrated together with a melt, the system being doped with a high enough concentration so that the element under study can be analysed with a microprobe. This technique can indicate how well an element has distributed itself in each phase. The main danger with this method is the use of element concentrations which are too high to obey Henry's law. An alternative to doping and electron microprobe analysis is phase separation by heavy liquids and hand picking. Problems will again arise from incomplete phase separation.

Radio-active isotopes of trace elements have also been used in multiphase systems. After the experiment the beta emissions

from these isotopes can be picked up by autoradiography. Mysen and Seitz (1974) describe the feasibility of using beta track mapping in measuring partition coefficients. This technique is useful over a wide range so that the effect of concentration on partition coefficients can be determined. The location of an element in a particular phase may also be obtained.

This study employed a double capsule technique used by Fung and Shaw (1978). Chlorite gel was placed in a small gold capsule which had the end crimped just enough to contain the chlorite. The vapor phase was still able to communicate with the chlorite. The capsule containing chlorite was placed in a larger capsule along with a Li solution and albite gel. This method enabled the chlorite and albite to be separated after the experiment. Since the density and color of Mg-chlorite is not very different from albite, mineral separation would have been very difficult without the double capsule technique. The Li can be measured by activation analysis using alpha recorders if boron is not present, otherwise atomic absorption can be used. With the small amount of vapor phase used in these experiments problems were encountered with its recovery and analysis. The Li distribution between albite and chlorite was not affected by this problem since the Li composition of the vapor was not required and it was not necessary to recover 100 % of each mineral for Li analysis.

CHAPTER II

EXPERIMENTS AND DATA PROCESSING

II-1 Experimental proceedure

In this study Li distribution between chlorite and albite in a common vapor phase was measured using a double capsule technique. See the appendix for details. Chlorite and albite were grown from synthetic gels prepared in a similar way to the method of Luth and Ingamells (1965). Details are given in the appendix.

Concentrations of Li added in solution did not exceed 1000 ppm, and were kept low so that Henry's law would be obeyed, and natural Li concentrations would be simulated. To measure the low Li concentrations an activation analysis was employed (See appendix,). When ^{6}Li is hit by a neutron an alpha particle is emitted and can be recorded on a cellulose nitrate film. The alpha tracks are revealed by etching and can be counted on the assumption of direct proportionality to Li concentration. Boron masks this Li reaction, therefore experiments were restricted to a boron-free system.

Atomic absorption was used to measure Li in solution and in the natural minerals which contained boron. Atomic absorption proceedures are described in the appendix.

Several experiments were conducted in which chlorite and

albite were crystallized from a single gel whose composition was inter-

mediate between the two minerals. No Li was used. The purpose of these

experiments was to demonstrate that chlorite and albite could grow

together in equilibrium. Experimental times were varied to determine

the time required to reach equilibrium.

Most experiments were started with separate gels of albite

and clinochlore composition. Lithium was introduced as a LiCl solution.

These experiments were conducted at 400^0, 500^0, 600^0, and 700^0 C to

determine the temperature dependance of Li distributions. Several

of these runs were held at one temperature for two weeks, quenched,

and then brought to equilibrium at a different temperature. This

would test how quickly Li distribution adjusts to a new temperature.

Another set of experiments was conducted in which Li was

included in the clinochlore gel. In the previous set Li was removed

from the solution by clinochlore, while these experiments measured

the leaching of Li from clinochlore gel. They serve as another test

of equilibrium since the Li distributions should be independant of the

way in which Li is introduced. Some of these runs used a 3 wt. % NaCl

solution and others used deionized water in an attempt to determine

the influence of vapor composition on Li partitioning.

A final set of experiments was carried out with natural

chlorite and albite. The albite was Ab-1 from Amelia County, Virginia,

and the chlorite was an iron-bearing variety from Whitefish Falls,

Ontario. A further description of these minerals is given in the appendix. These experiments tested the effect of using already cristalline material to measure Li distribution. The presence of iron added a further complication to the Li distributions. The oxygen fugacity was buffered with Ni-NiO as described in the appendix.

II-2 Analytical errors

Errors in the atomic absorption analysis of Li are shown in table II-1, which gives the measured Li values for several international standard reference samples. These were analysed at the same time as the Li-standard gels and the minerals from the iron-chlorite experiments. Since the standards had a range in major element composition (basalt-granite), matrix interferences should become apparent. For example, Slate T3 appears slightly low in Li while the granite and basalts were high. Averaged Li values and standard deviations from separate analyses are given below.

standard	average Li (ppm)	% standard deviation
slate T3	110 ± 3	3
basalt BM	77 ± 5	6
basalt BR	14.5 ± 0.7	5
granite GH	45 ± 4	9

During a particular Li analysis instrumental variation was usually 1 to 6 %. When concentrations were very low this variation was as high as 20 %. Instrumental variation for the analysis of Mg, Fe, and Na is usually better than 1 %, while Al was better than 10 %.

16

Table II-1

date	standard	measured	published (Abbey)	$\dfrac{\text{measured} - \text{Abbey}}{\text{Abbey}} \times 100$
July 23/79	slate T3	107 ± 1	115	- 7
" " "	basalt 3M	78	70	11
" " "	basalt 3R	14	12	17
Oct. 24/79	slate T3	109 ± 1	115	- 5
" " "	basalt 3M	79 ± 1	70	13
" " "	basalt 3R	15	12	23
Nov. 3/79	granite GH	48 ± 1	42	14
" " "	slate T3	113 ± 1	115	- 2
" " "	basalt 3R	82 ± 1	70	17
Aug. 3/80	granite GH	42	42	0
" " "	basalt 3M	70	70	0

In flame mode .014 ppm Li could be detected in solution, while the graphite furnace could detect .004 ppm. The mineral concentrations represented by these values depend on the weight of sample dissolved and the amount of solution which contains the sample. Table II-2 gives possible detection limits of lithium in the minerals. In several cases the amount of albite which could be analysed was only .001 gm, so that 20 ppm was a detection limit.

Table II-2

Lithium Detection Limits

	flame detects .014 ppm	furnace detects .004 ppm
given a solution wt. of 5 gm:	.070 μg	.020 μg
given a sample wt. of .001 gm:	70 ppm	20 ppm
given a sample wt. of .005 gm:	14 ppm	4 ppm

Errors in the activation analysis can be illustrated with figure II-1, which shows the calibration line for sample group P. For comparison, other calibration lines are given in figure A-1 in the appendix. The averaged alpha-counts of the Li standards are plotted as well as the averaged alpha-counts of the samples in group P. The vertical error bars show the 90 % confidence interval of the mean alpha-counts given by:

$$t_{\alpha/2} \times s/\sqrt{n}$$

where: s = standard deviation

n = sample number

$t_{\alpha/2}$ = t statistic for $\alpha = 0.10$

The dotted lines in figure II-1 represent the 90 % confidence interval of the mean response of alpha-counts to a given ppm Li. The error of the mean alpha-counts for a given sample can be less than or greater than this confidence interval. To estimate the error on each sample the error of the mean alpha-counts will be used since it varies from sample to sample. These errors are shown for each sample in table A-2 in the appendix and converted to ppm Li. The average errors for

Figure II-1 Calibration line for sample group P. Standards $(+)$ and
samples $(\oplus)$ have error bars representing the 90 % confidence interval
of the mean response. The dashed line represents the 90 % confidence
interval of the mean response of alpha counts to a given ppm Li. The
detection limit (alpha counts/mm^2) is given by the Y intercept of the
upper dashed line. The 90 % confidence interval of the mean response
of alpha counts to a given ppm Li is given by:

$$t_{\alpha/2}\ S\sqrt{1/n + (x_o - \overline{x})^2/S_{xx}}$$

x_o = ppm Li in standard at which confidence interval was
       calculated

$\overline{x}$ = mean ppm Li in standards

n = number of counts

$$S_{xx} = \sum_{i=1}^{n} (x_i - \overline{x})^2$$

S = standard deviation reflecting variation about the
     regression line

$t_{\alpha/2}$ = t distribution with $n - 2$ degrees of freedom
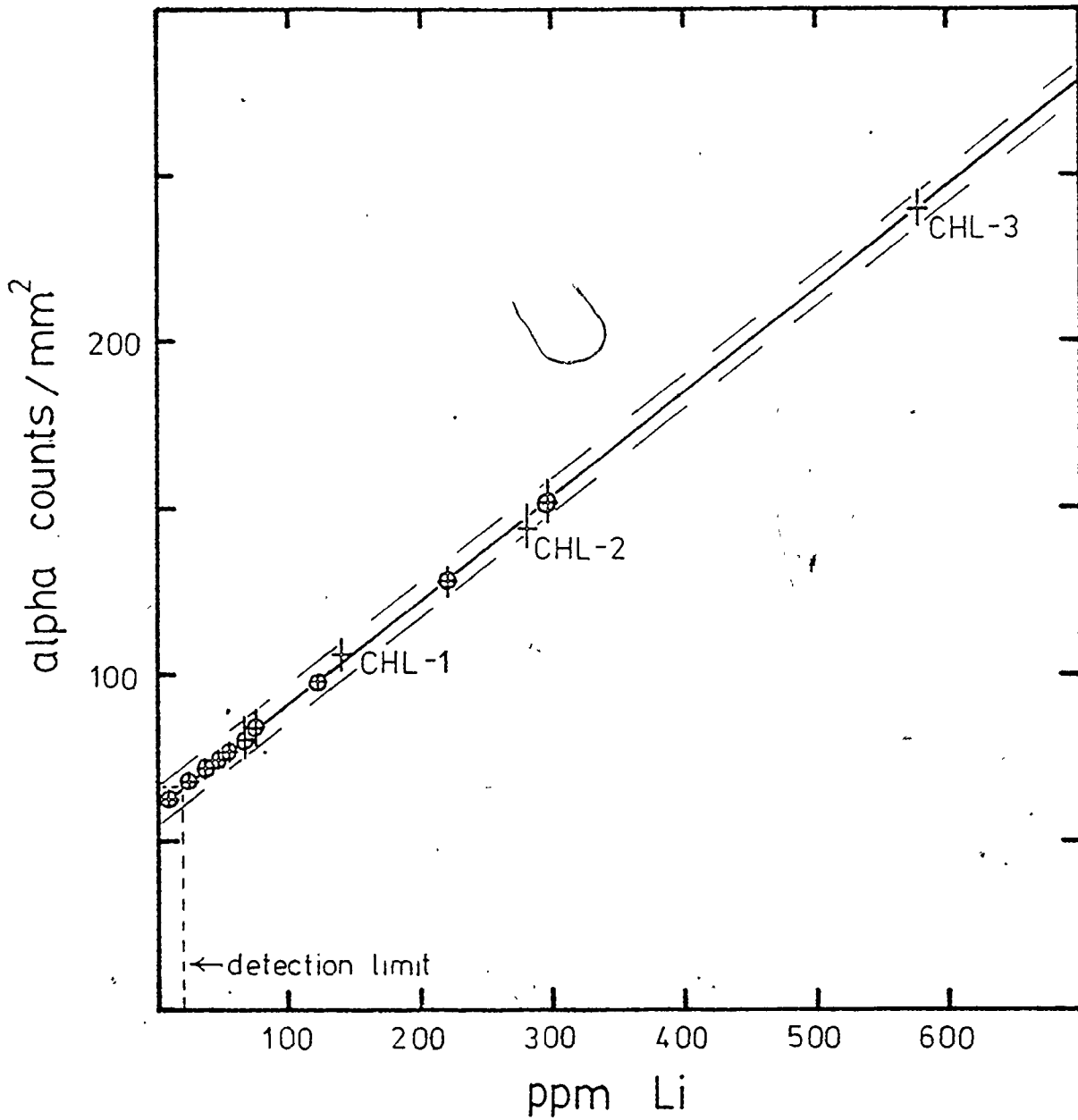
ppm Li in albite and chlorite are 14 and 19 respectively, with standard
deviations of 5 and 9.

The detection limit is the Li concentration above which
the calibration line can confidently detect Li. Detection limits for
each sample group are given in table II-3. They were calculated assum-
ing that at 0 ppm Li the alpha-count could be higher by the 90 % con-
fidence interval of the mean response such as shown by the dashed line
in figure II-1. This error was divided by the slope of the calibration
curve to give the limit of detection. The detection limit is different
for each sample group and if more low Li standards are used it could
be reduced.

Table II-3

sample group	detection limit (ppm Li)
F	5
I	4
G	9
M	7
N	15
O	13
P	17
Q	10

II-3 Experimental errors

This section will briefly describe potential sources of error that could be introduced during the loading of gold capsules, the hydrothermal synthesis, and the opening of gold capsules.

Loss of Li solution could have occurred during the welding of gold capsules. If the recorded weight losses during welding were not due to volatilized gold as suggested in the appendix by the section on experimental proceedure the amount of Li lost may be 5 to 10 % in some cases.

During the experiment errors may have been introduced by incomplete equilibration due to poor circulation of the vapor phase between chlorite and albite. The section on experimental procedure in the appendix describes how to deal with the possibility of Li vapor leaking from the capsule and the danger of Li adsorbing to the minerals after the experiments are quenched. The Li distributions may be affected by the grain size of the solid phases and by the nature of the starting material. Experiments started with synthetic gels may give different results from ones using natural minerals in which crystal bonds may have to be broken or Li may have to diffuse into a crystal structure.

During the opening of the gold capsules Li-containing solution may be trapped in the scrap gold. To reduce this problem the gold scraps were boiled as described in the experimental proceedure. During the recovery of the vapor phase there was a good possibility that Li was lost by adsorption to filter paper and/or the glass walls of the

beaker and Millipore filter system. Experiments showed that filter paper adsorbed Li and retained it after washing with deionized water. If 0.02 gm of a 100 ppm "vapor" solution are diluted to 100 gm the resulting Li concentration would be 0.02 ppm. The Li content of such a dilute solution could be seriously affected by Li loss due to adsorption.

II-4 Li mass balance and calculation of vapor composition

A lithium mass balance calculation was made for each sample to determine the amount of Li which could be accounted for. This calculation served as a check on the measured concentration of Li in the vapor phase, which was particularly sensitive to errors.

The mass balance calculation is summarized in table II-4. The μg of Li in each mineral were calculated from the mineral's measured Li concentration and its mass. The original mass of chlorite had to be increased to allow for water uptake from the vapor, and the mass of vapor was adjusted to compensate for this loss. The initial μg Li was the amount of Li added to the system by solution or in the chlorite-gel. If a solution loss was suspected during welding the initial μg Li was adjusted by calculating the percentage of solution lost and reducing the μg Li by this percentage.

Column 4, μg Li left, is the difference between the initial μg Li (column 3) and the total Li in the minerals (the sum of columns 1 and 2). When this value is compared to the μg Li measured in solution (column 5) significant loss is apparent in most cases. Among the possible causes of Li loss discussed under experimental errors, the

loss due to adsorption onto filter paper and glass may be very impor-
tant. There is also a possibility that a small amount of a Li-rich
phase formed and was not detected. In a few cases the measured Li was
greater than the μg Li left. This might be attributed to errors in the
Li concentrations and the mineral weights, or the separated solution
could have been contaminated with small amounts of the mineral phase,
which gave up their Li when the samples were acidified for storage.

Due to the large differences between columns 4 and 5 con-
siderable doubt arises as to which or any of these columns represents
the true amount of Li in the vapor phase. Therefore, further discussion
of Li in the vapor phase will be left to the·appendix.

Table II- 4

Li mass balance and calculation of vapor composition

	1	2	3	4	5	6	7
	μg Li in chlorite	μg Li in albite	initial μg Li	μg Li left	measured μg Li in solution	mass of vapor	ppm Li in vapor
C-1	7.994	3.158	16.80	5.648	0.795	.0150	377
C-3	2.242	0.872	5.90	2.786	2.342	.0100	869
C-4	2.296	0.804	4.00	0.900	0.293	.0054	167
C-5	1.919	1.241	5.08	1.920	1.563	.0111	173
C-6	8.942	4.976	22.40	8.482	0.280	.0206	412
C-7	2.196	1.366	9.200	5.637	4.271	.0166	340
c-8	9.827	4.043	24.10	10.23	2.031	.0222	461
C-10	8.231	6.199	24.80	10.37	0.882	.0228	455
C-11	0.765	0.415	10.75	9.570	0.172	.0193	496
C-12	2.673	0.800	14.65	11.18	0.395	.0272	411
C-13	1.827	1.008	6.875	4.040	0.812	.0256	158
C-14	2.153	1.415	5.600	2.032	0.448	.0204	100
C-15	3.658	2.309	13.85	7.883	8.755	.0259	304
C-16	0.942	0.374	24.80	23.48	15.92	.0234	1030
C-19	3.762	1.072	25.70	20.87	7.404	.0265	892
C-20	1.711	0.938	14.45	11.80	0.098	.0225	445
C-21	6.682	2.531	12.50	3.287	0.381	.0223	146
C-24	5.251	3.844	18.20	9.105	2.906	.0159	573
C-25	1.279	0.690	11.40	9.431	0.273	.0207	456
C-26	4.986	3.448	10.40	1.967	1.498	.0186	106
C-27	2.016	0.935	11.90	8.949	3.362	.0216	414
C-28	4.355	3.774	12.60	4.471	1.292	.0289	155
C-29	0.688	0.037	4.933	4.208	6.922	.0169	249
C-30	1.339	0.670	4.781	2.772	1.824	.0156	178
C-31	1.104	0.615	5.312	3.593	0.882	.0176	204
C-32	1.151	0.555	5.684	3.979	1.646	.0191	208

Table II-4 Continued

	1	2	3	4	5	6	7
	μg Li in chlorite	μg Li in albite	initial μg Li	μg Li left	measured μg Li in solution	mass of vapor	ppm Li in vapor
C-33	0.439	0.592	5.524	4.493	0.142	.0184	244
C-34	2.739	1.270	6.188	2.179	0.147	.0210	104
C-35	6.549	1.997	11.55	3.004	0.421	.0209	144
C-36	4.690	1.320	10.90	4.890	0.151	.0195	251
C-37	3.500	0.718	10.50	6.282	2.852	.0184	341
C-38	3.571	2.058	6.405	0.776	0.789	.0254	31
C-39	1.605	0.493	5.943	3.845	0.512	.0248	155
C-40	2.656	0.980	5.828	2.192	1.441	.0256	86
C-41	1.316	0.915	6.462	4.231	4.945	.0202	209
C-42	1.026	0.454	5.712	4.232	4.021	.0165	256
C-43	1.661	0.533	4.847	2.653	2.483	.0286	157
C-46	3.178	1.826	14.57	9.566	2.628	.0120	797
C-47	2.706	1.044	15.76	12.01	4.671	.0190	632
C-48	6.960	4.104	15.04	3.977	4.215	.0339	118
C-49	2.293	1.115	32.40	28.99	0.165	.0300	966
C-60	5.945	2.510	34.40	25.95	1.066	.0321	808
C-61	7.440	3.146	21.70	11.12	4.085	.0195	570
	μg Li in minerals						
C-53	3.840		25.23	21.39	4.517	.0479	447
C-54	3.670		25.82	22.15	5.751	.0448	494
C-56	4.879		24.02	19.15	4.120	.0572	335
C-57	6.711		9.408	2.697	3.291	.0448	73
C-58	2.384		8.589	6.205	2.079	.0541	115
C-59	11.76		39.90	28.14	30.00	.0399	752
C-65	10.14		43.06	32.92	26.28	.0488	675

CHAPTER III

DATA AND DATA EVALUATION

III-1 Was equilibrium achieved?

An attempt was made to grow chlorite and albite from homogeneous starting material. The experiment was conducted at 500^0 C and at various experimental times varying from 168 to 1,032 hours. The experimental products were collected on filter paper in the usual manner and X-rayed. The diffractograms were not very good because of the small sample size. Measured d-spacings were adjusted to a quartz standard and were compared to published values. Chlorite and albite peaks appeared and became more distinct with longer reaction time (see table III-1). A minimum of 672 hours (28 days) appears to be required to develop good crystals at 500^0 C.

The distribution coefficient, $D^{alb-chl}$, was plotted against reaction time in figure III-1. The object of this exercise was to see if there was a change in Li distribution between albite and chlorite with reaction time. If a change became obvious then the reaction was too short to achieve equilibrium. No covariation between $D^{alb-chl}$ and time was found and the coefficient of determination (r^2) showed that only 10 % of the variation of $D^{alb-chl}$ was explained by a linear variation with time. Therefore, reaction times of 697 hours were long enough to

Table III-1

Diffractograms of albite and chlorite grown from the same gel

	E-7	E-8	E-6		E-5	
experiment time (hr.)	168	360	672		1,032	
chlorite		14.79	14.82	(40)	14.50	(50)
	7.570		7.36	(40)	7.37	(63)
			4.91	(70)	4.88	(100)
	4.562	4.537	4.584	(100)	4.546	(38)
					3.259	(38)
			2.560	(40)	2.555	(38)
					2.399	(50)
albite	4.001 (25)	3.996	3.996	(50)	3.997	(40)
			3.847	(8)		
	3.740 (25)	3.705	3.715	(34)	3.726	(30)
			3.619	(14)	3.609	(35)
	3.187 (100)	3.186	3.184	(100)	3.179	(100)
			3.111	(8)		
			2.938	(12)	2.938	(30)
		2.631	2.627	(10)	2.627	(15)
unknown	15.17					
	5.035	5.026				
	3.030	3.036				

- D spacings are given in angstroms.

- Relative peak intensities are given as percentages by numbers in brackets.

Figure III-1 The individual lithium partition coefficients
between albite and chlorite at 500^0 C are plotted against reaction
time. Error bars were not shown since they would mask the data points
as can be shown by inspection of calculated errors given in table III-3.
Note that the point with a D value of 1.75 has a 116 % error. As is
shown by r^2 = 0.10 there is very little linear covariation between
D values and reaction time.
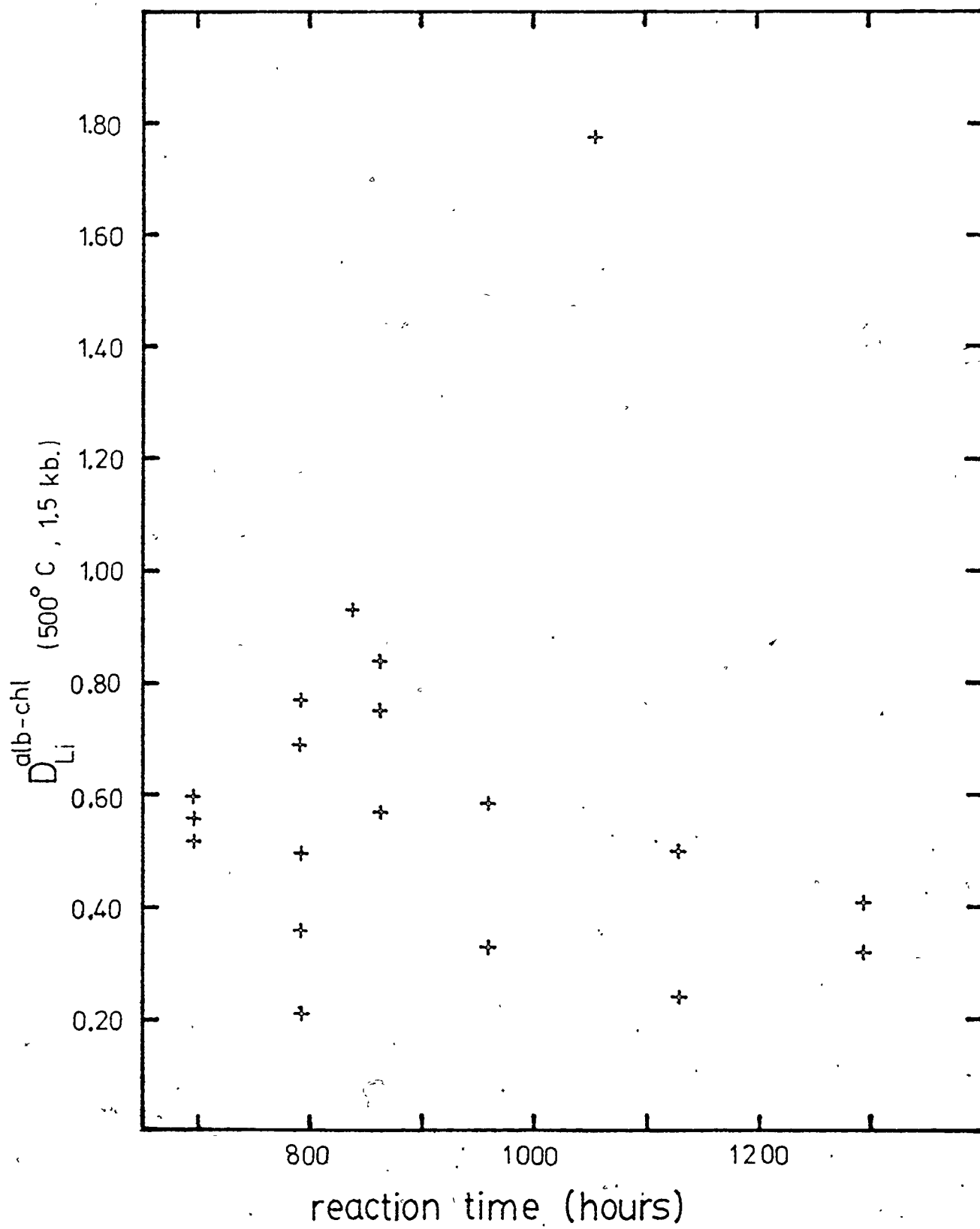
achieve equilibrium at 500^0 C. At higher temperatures shorter times would be required. The shortest reaction time at 600^0 C and 700^0 C was 792 hours which should have been adequate to achieve equilibrium. Since the reaction kinetics would be slower at 400^0 C the experimental time was almost doubled to 1320 and 1470 hours.

Iiyama (1974) conducted reversal experiments on Na, K, Rb, Cs, Sr and Ba exchange between aqueous solution and feldspar at 600^0 C. He found that equilibrium was achieved in 10 days (240 hours). Fung (1978) found that exchange isotherms of Rb, Tl and K between sanidine and vapor remained constant after 14 days (336 hours). Volfinger et Robert (1979) measured Li exchange between phlogopite and vapor at 600^0 C using an experimental time of 10 to 30 days (720 hours).

In conclusion, the reaction times used in this study are probably long enough to have achieved equilibrium.

To test whether Li was able to equilibrate between chlorite, albite and the solution some experiments were started with a Li-chlorite-gel and a Li-free solution. If Li is able to exchange freely between chlorite (contained in the small capsule) and solution, these experiments should give the same results as those which had Li added in solution only. The Li-gels used were CHL-3 (576 ppm Li) and CHL-5 (1194 ppm Li).

Table III-2 gives the averaged distribution coefficients at 500^0 C, calculated from the coefficients shown in table III-3. Table III-2 compares the average $D^{alb-chl}$ for (1) all experiments at 500^0 C,

(2) the experiments in which Li is introduced in the chlorite, and

(3) the runs in which Li was added in the vapor. At first glance it
appears that the chlorite grown from a Li-gel prefers to retain slightly
more Li than the chlorites grown in a Li solution. This is also shown by
a plot of Li in albite versus Li in chlorite (figure III-3)[*]. However,
the difference in distribution coefficients produced by the two sets
of experiments is not very large since their standard deviations overlap
and the difference was not significant at the 99 % confidence interval
(table III-5). This is further evidence that equilibrium was achieved
in these experiments.

Table III-2

Average distribution coefficients

	$D^{alb-chl}$	sample number
total at 500^0 C	0.57 ± 0.34	21
Li started in chlorite	0.37 ± 0.15	13
Li started in solution	0.70 ± 0.36	8

Given errors are standard deviations.

III-2 Lithium distributions

Lithium concentrations in albite and chlorite are summarized
in table III-3 and partition coefficients are calculated for each
experiment. Table III-4 gives the averaged Li distribution for each
group in table III-3. When the standard deviations in table III-4 are
compared to those of the vapor-mineral distributions in the appendix
(table A-10) it becomes clear that partition coefficients measured

* Figure III-3 is found on page 36, in the discussion of the temperature
dependence of D values.

Table III-3

Lithium distributions

sample	ppm Li albite	ppm Li chlorite	$D^{alb-chl}$	possible % error	reaction time (hrs)	
			temperature	500^0C		
1	319	571	0.56	10	696	
3	83	159	0.53	18	696	
4	67	112	0.60	31	696	
5	107	156	0.69	20	792	
7	122	158	0.77	18	792	
19	67	209	0.32	23	1296	
21	143	348	0.41	18	1296	
24	248	295	0.84	14	864	
26	221	295	0.75	17	864	
28	222	238	0.93	20	840	
29	15	37	0.41	27	1056	
31	34	60	0.57	60	864	
33	42	24	1.75	116	840	
38	140	279	0.50	15	792	LIC
39	28	136	0.21	30	792	LIC
40	56	229	0.24	29	1128	LIC
41	52	102	0.51	72	1128	LIC
42	32	90	0.36	19	792	LIC
43	36	173	0.21	43	792	LIC
47	59	178	0.33	12	959	LIC
48	283	480	0.59	12	959	LIC

Table III-3 continued

sample	ppm Li albite	ppm Li chlorite	$D^{alb-chl}$	possible % error	reaction time (hrs)
		temperature	500^0 C	(natural minerals)	
53	63	148	0.43	11	1056
54	45	135	0.33	11	1056
56	54	148	0.36	11	1056
57	184	144	1.28	11	1056
58	16	105	0.15	11	984
59	338	240	1.41	11	984
65	254	148	1.72	11	984
		temperature	400^0 C		
10	574	538	1.07	9	1470
12	80	164	0.60	53	1470
13	60	126	0.48	63	1470
14	122	138	0.88	35	1460
15	222	267	0.83	13	1470
16	21	62	0.34	90	1468
27	55	120	0.46	37	1320
32	30	65	0.46	22	1320
		temperature	600^0 C		
6	319	648	0.49	10	792
8	304	664	0.46	6	792
11	34	45	0.76	67	818
20	83	93	0.89	59	812
25	35	78	0.45	95	912
30	37	72	0.51	17	912
34	73	153	0.48	20	912
36	83	268	0.31	31	912
46	112	227	0.49	25	842	LIC
49	78	126	0.62	19	842

Table III-3 continued

sample	ppm Li albite	ppm Li chlorite	$D^{alb-chl}$	possible % error	reaction time (hrs)
temperature 700° C					
35	104	383	0.27	17	792
37	39	175	0.22	21	792
60	163	334	0.49	19	865
61	207	435	0.48	10	865

possible % error: This represents the uncertainty in the individual Li analysis and is given by the sum of the % error of Li in albite and in chlorite.

LIC: Represents those experiments in which Li started in the chlorite gel.

Table III- 4

Averaged lithium distributions

group	$D^{alb-chl}$	standard deviation	error of the mean	n
400° C	0.64	0.26	0.17	8
500° C	0.57	0.34	0.13	21
600° C	0.55	0.17	0.10	10
700° C	0.37	0.14	0.15	4
mean	0.56	0.23	0.06	43
natural minerals	0.81	0.64	0.46	7

error of the mean = $t_{\alpha/2} \cdot s / n$ (Walpole and Myers, 1972)

where: $\alpha = 0.10$

s = standard deviation

Table III-5

t statistic for two means

μ = mean $D^{alb-chl}$ at given temperature

null hypothesis (H_o): $\mu_1 - \mu_2 = 0$

alternate hypothesis (H_1): $\mu_1 < \mu_2$

α = 0.10 and 0.01

1	2	critical region		computed T	degrees of freedom	conclusion: accept	
		α=.10	α=.01			α=.10	α=.01
500^0 C	600^0 C	1.311	2.462	0.253	29	H_o	H_o
400^0 C	500^0 C	1.314	2.473	0.493	27	H_o	H_o
500^0 C	700^0 C	1.319	2.500	1.206	23	H_o	H_o
500^0 C Fe-chl	500^0 C Mg-chl	1.315	2.479	1.278	26	H_o	H_o
Li from solution	Li from chlorite	1.328	2.539	2.455	19	H_1	H_o

Critical values for the T distribution were taken from Walpole and Myers (1972). The T statistic was calculated assuming that the sample populations were normally distributed with the same unknown variance.

$$T = (x_1 - x_2)/S_p\sqrt{(1/n_1) + (1/n_2)}$$
$$S_p^2 = ((n_1 - 1)S_1^2 + (n_2 - 1)S_2^2)/(n_1 + n_2 - 2)$$

degrees of freedom: $v = n_1 + n_2 - 2$.

If the calculated value exceeded the critical value the null hypothesis was rejected and one Li distribution was accepted as being significantly higher than the other.

between vapor and minerals are much less precise than those between albite and chlorite.

Although the largest group of experiments was conducted at 500^0 C, a number of experiments at 400^0, 600^0 and 700^0 C could be used to evaluate the effect of temperature on Li partitioning. To determine whether the Li distributions vary with temperature, the average distribution coefficients for each temperature will be compared. Li distribution plots for each temperature are shown in figures III-2 to III- 4.

When table III- 4 is examined the lithium distributions between albite and chlorite do not seem to vary significantly with temperature. This was confirmed by table III-5 which showed that $D^{alb-chl}$ at 500^0 C was not significantly different from the $D^{alb-chl}$ at 400^0, 600^0 and 700^0 C at the 99 % confidence interval.

The plots of Li in albite versus Li in chlorite (figures III 2 to 5) indicated that the lithium distributions could be linear. Therefore, linear regression models were calculated for each temperature. In each case the regression line did not pass through the origin, although for 500^0, 600^0 and 700^0 C, the origin does fall within the error limits of the Y intercept. The regression line at 400^0 C stands out from the others. It has a significantly higher slope, and may be curved near the origin. However, this curve may be unduly influenced by point 10. Also, the slope of this line (1.17 ± 0.12) is significantly different from the average $D^{alb-chl}$ at 400^0 C (0.64 ± 0.26). The slopes

Figure III-2 Li in albite plotted against Li in chlorite at 400^0 C.
Dashed lines represent the 90 % confidence interval for a single
response. Regression coefficients were:

$$a_0 = -71 \pm 29$$
$$a_1 = 1.17 \pm 0.12 \quad [D^{alb-chl}]$$
$$r^2 = 0.98$$

Regression equation: ppm Li in albite = $a_0 + a_1$(ppm Li in chlorite)

Crosses represent errors in Li analysis (table A-5, p 70).

Experiment 10 is referred to in the text.
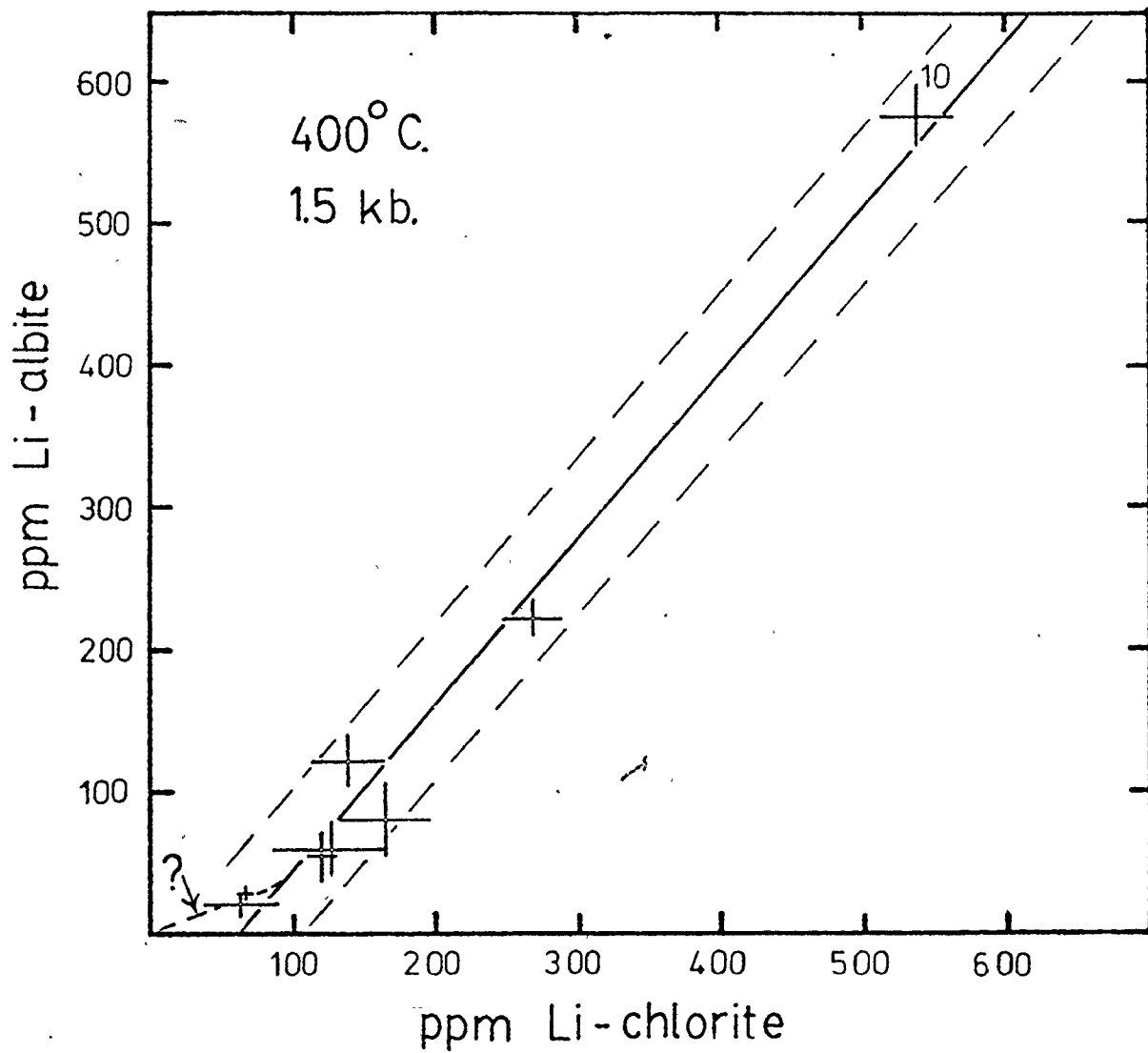
Figure III-3 Li in albite plotted against Li in chlorite.at 500^0 C.
Dashed lines represent the 90 % confidence interval for a single
response. Regression coefficients were:

$a_o = -10. \pm 31$

$a_1 = 0.59 \pm 0.13$ $[D^{alb-chl}]$

$r^2 = 0.78$

⊕ : samples in which Li started in chlorite

╂ : samples in which Li started in solution
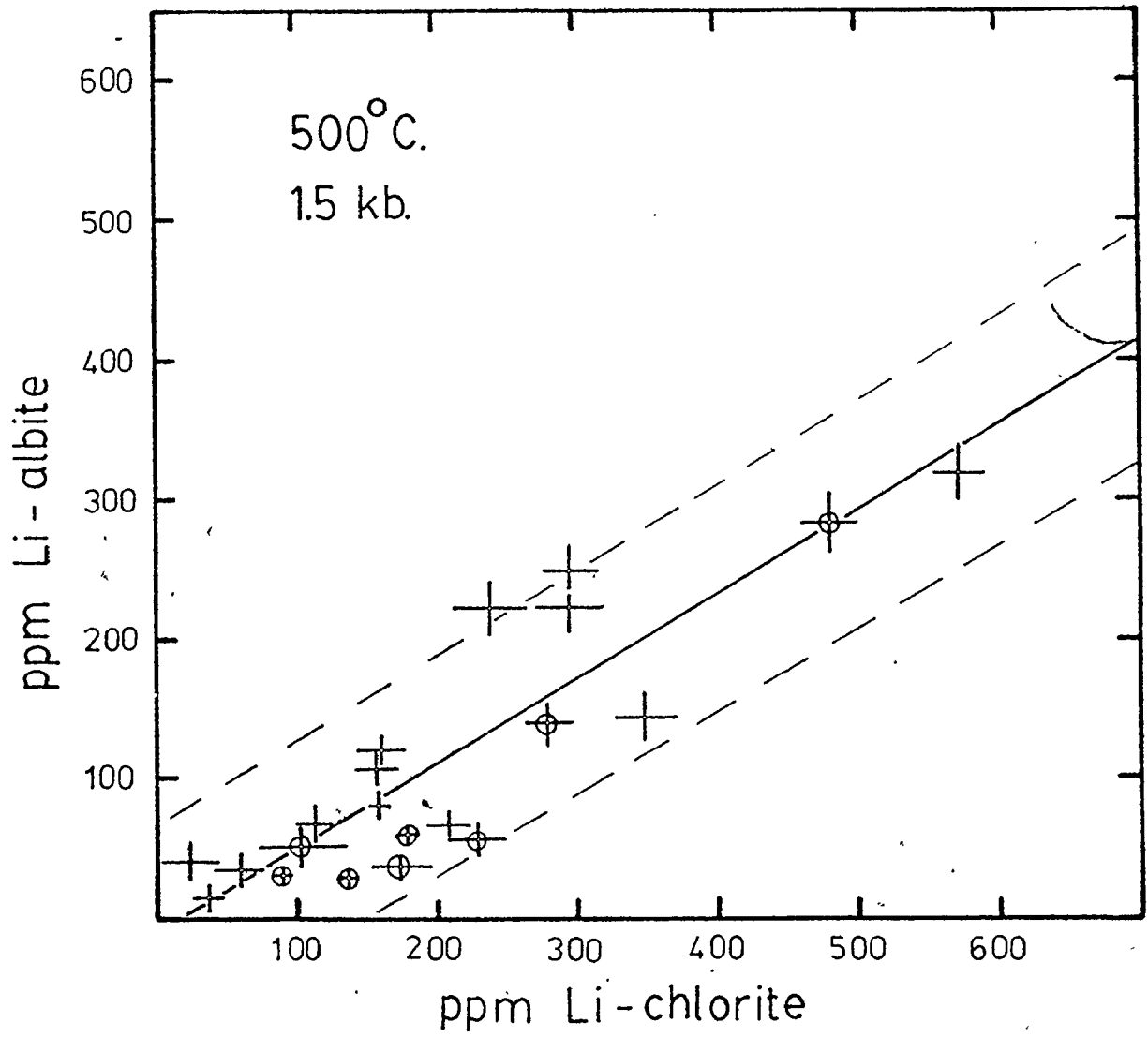
Figure III-4 Li in albite plotted against Li in chlorite at
600^0 C. Dashed lines represent the 90 % confidence interval for
a single response. Regression coefficients were:

$$a_o = 9 \pm 19$$
$$a_1 = 0.45 \pm 0.06 \quad [D^{alb-chl}]$$
$$r^2 = 0.96$$

600°C.
1.5 kb.
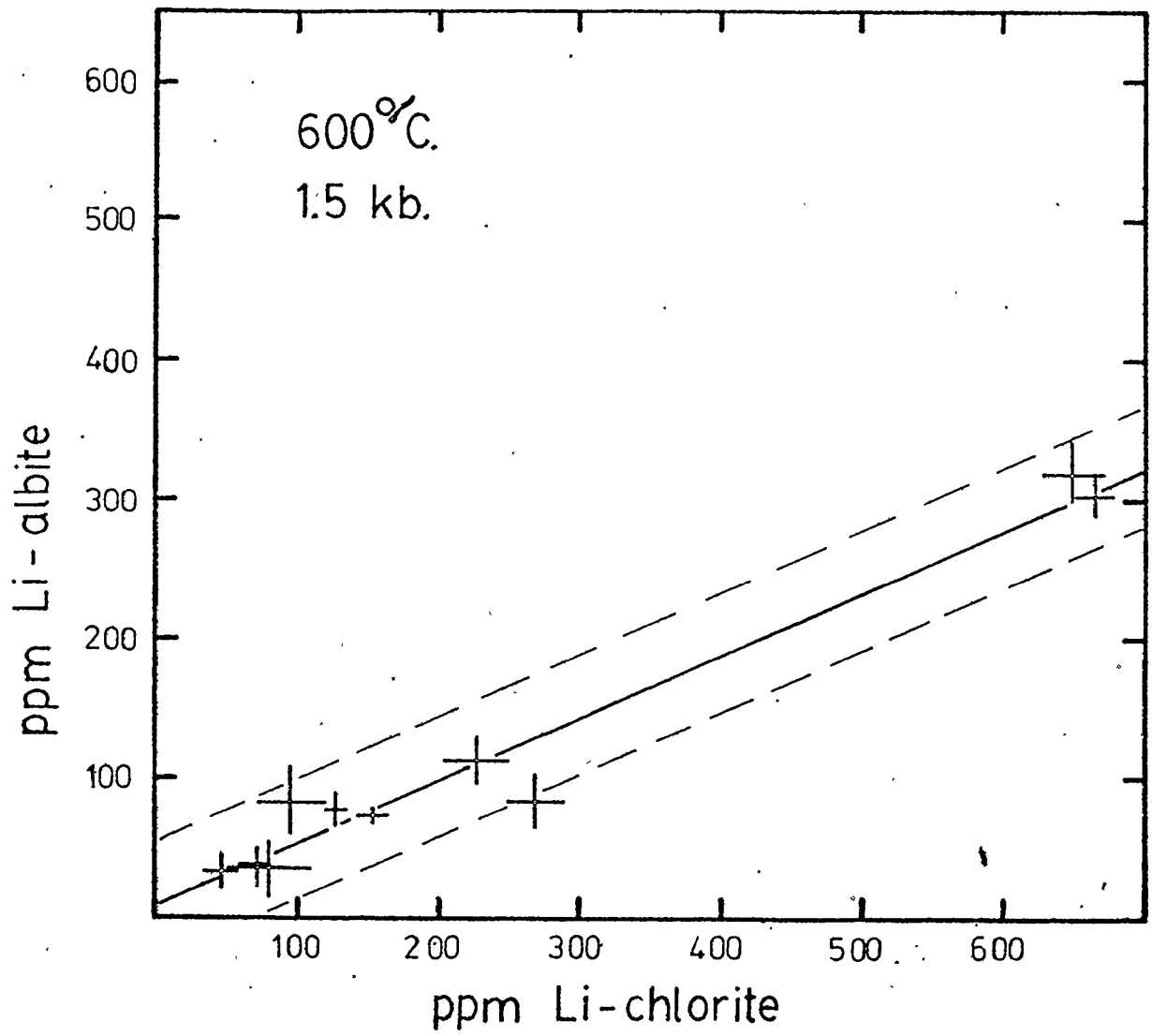
Figure III-5 Li in albite plotted against Li in chlorite at 700^0 C. Dashed lines represent the 90 % confidence interval for a single response. Regression coefficients were:

$$a_o = - 55 \pm 178$$
$$a_1 = 0.55 \pm 0.52 \quad D^{alb-chl}$$
$$r^2 = 0.73$$
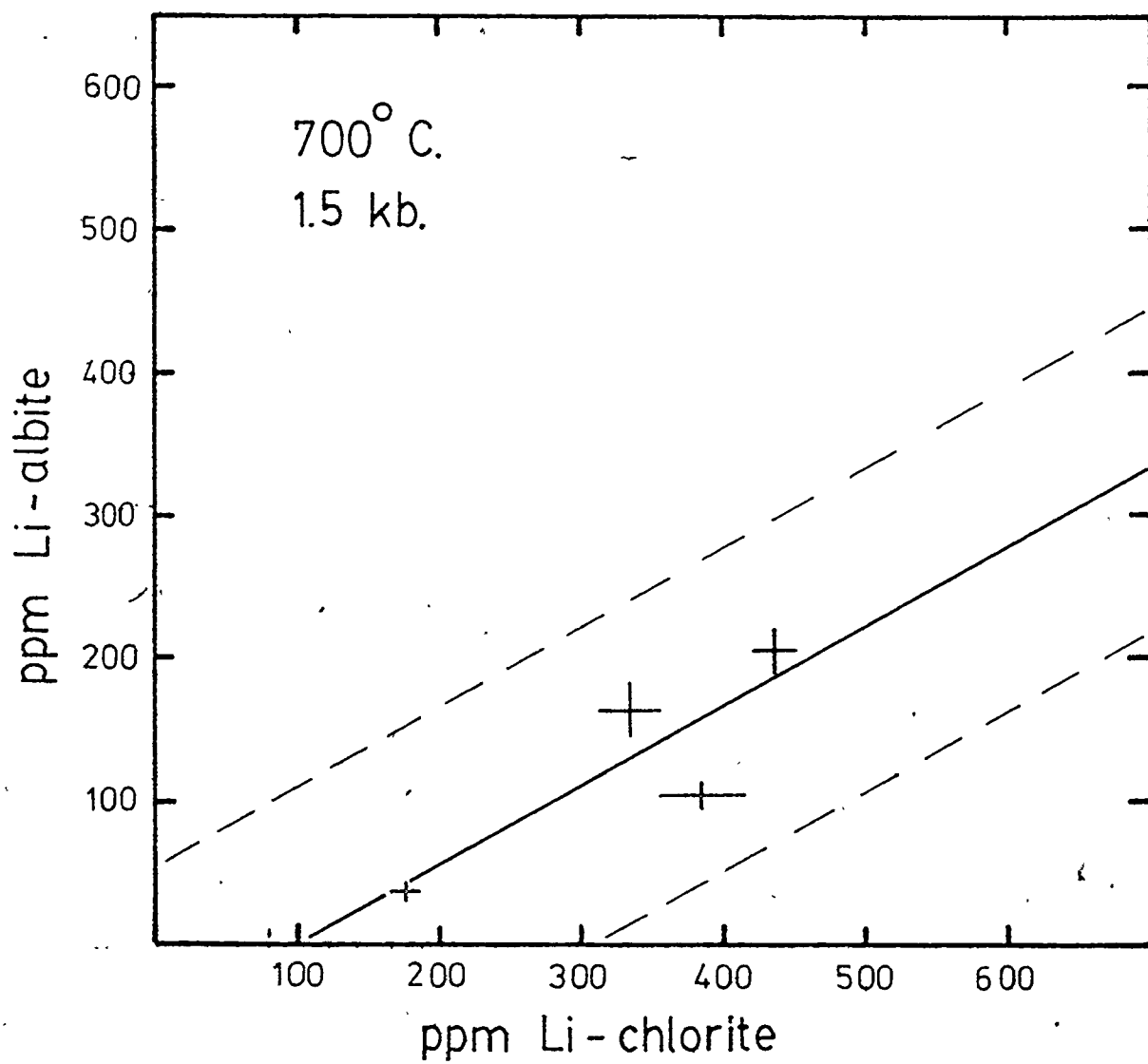
Figure III-6 Li in albite plotted against Li in chlorite at all

temperatures. . Dashed lines represent the 90 % confidence interval

for a single response. Regression coefficients were:

$$a_o = -8 \pm 20$$

$$a_1 = 0.582 \pm 0.073 \ [D^{alb-chl}]$$

$$r^2 = 0.72$$

$\times$ 400° c

$+$ 500° c

$\odot$ 600° c

$\diamondsuit$ 700° c
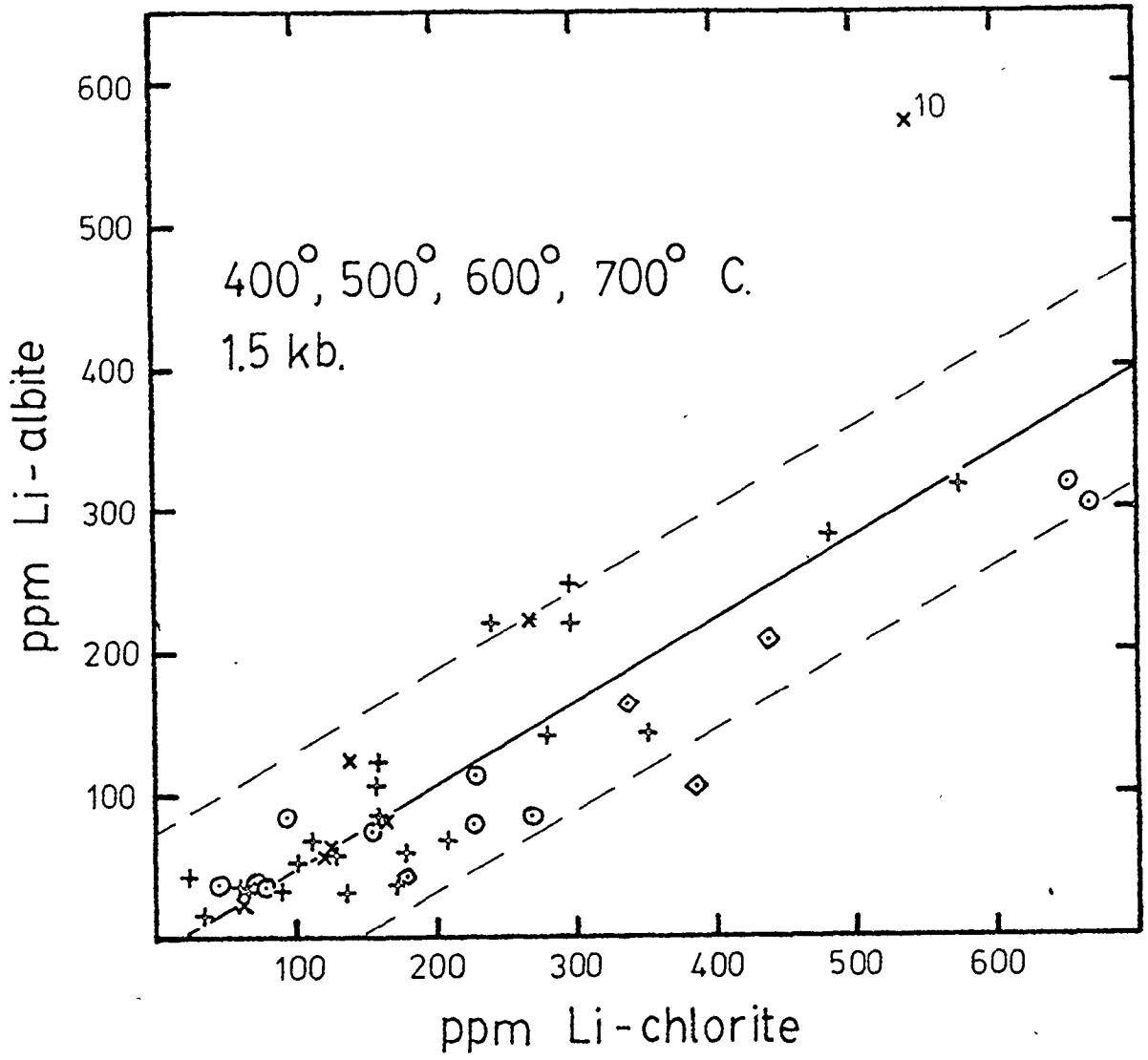
Figure III-7 Li in albite (Ab-1) versus Li in chlorite from Whitefish Falls equilibrated at 500^0 C. One regression line was calculated for all the points and another line was calculated for points 53, 54, 56, and 58. Dashed lines represent the 90 % confidence interval of the mean response. The regression coefficients were:

all points

$a_o = -228 \pm 237$

$a_1 = 2.39 \pm 1.51$

$r^2 = 0.65$

points 53, 54, 56, 58

$a_o = -88 \pm 36$

$a_1 = 0.99 \pm 0.27$

$r^2 = 0.97$
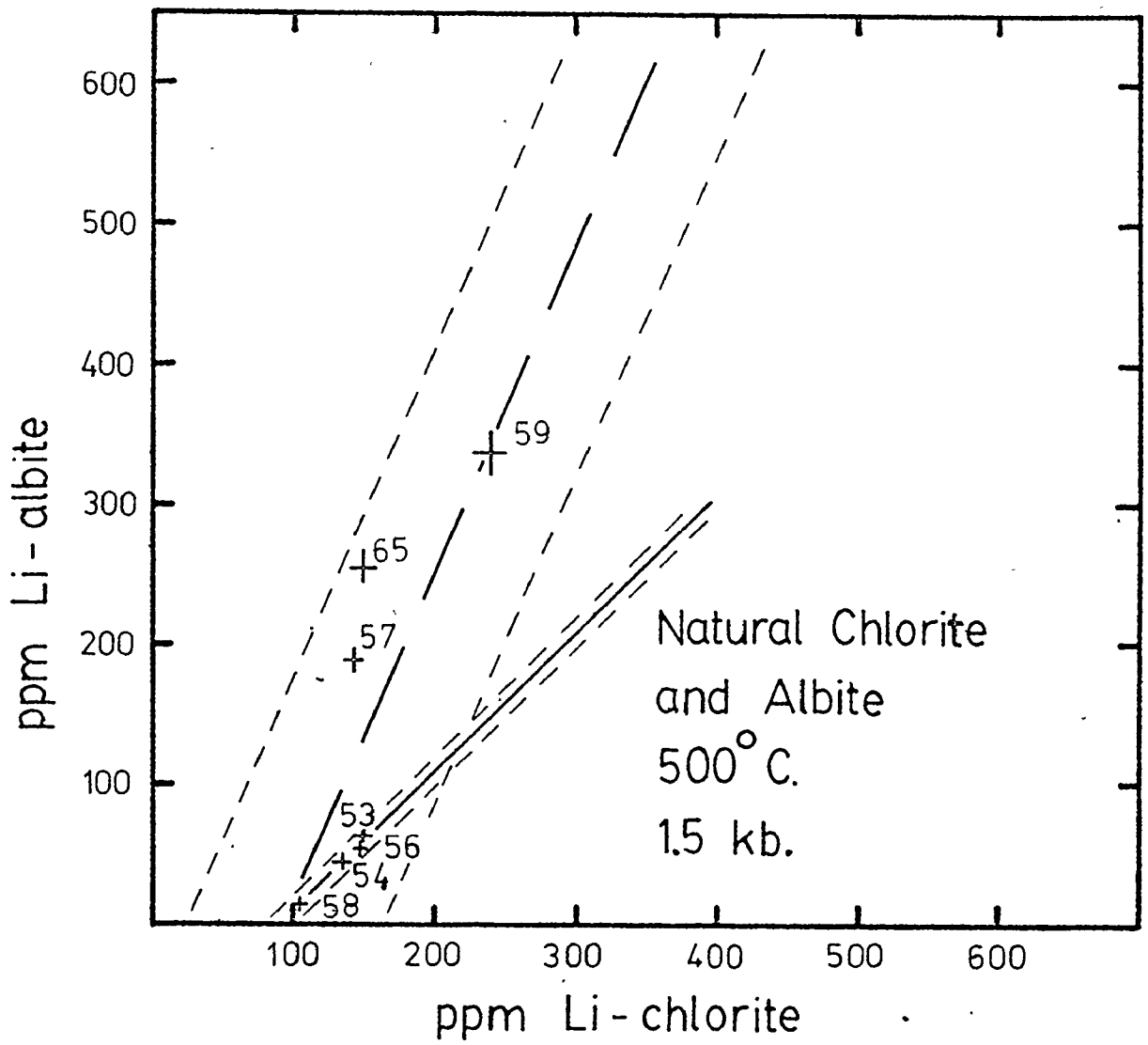
of the other lines do not significantly differ from the average Li distributions. The slopes at 500^0, 600^0 and 700^0 C fall within each other's error limits.

Since the average Li distributions between albite and chlorite at different temperatures were not significantly different, all the data were pooled into one distribution plot (figure III-6). The slope of this regression line was 0.582 ± 0.073 and the Y intercept was -8 ± 20. Seventy-two percent of the variation of Li in albite can be explained by a linear variation with Li in chlorite ($r^2 = 0.72$). Note that point 10 is significantly different. Since every other point at 400^0 C falls within the 90 % confidence interval for a single response, point 10 appears to be the only reason why the regression line for 400^0 C (figure III-2) is different from the others (figures III 3 to 5).

The Y intercept is not significantly different from zero, as would be expected if the chemical potential of Li was the same in albite and chlorite. The slope of the line is not significantly different from the average $D^{alb-chl}$ from all experiments with Mg-chlorite ($D^{alb-chl} = 0.56 \pm 0.06$).

In summary, the Li distribution between albite and chlorite is not significantly sensitive to temperature between 400^0 and 700^0 C. Since figure III-6 seems to indicate that Li partitioning is linear, Henry's law appears to be obeyed up to concentrations of at least 700 ppm Li in chlorite.

To determine the effect of using natural minerals on the measurement of Li partitioning an experiment was carried out using natural albite (Ab-1) and natural chlorite from Whitefish Falls, Ontario. A further complication was the presence of iron in the chlorite.

The average Li distribution from this experiment is shown in table III-4. Table III-5 evaluates the statistical significance of the difference between this $D^{alb-chl}$ and the average $D^{alb-chl}$ measured in the iron-free system at 500^0 C. In the natural system $D^{alb-chl}$ was not significantly higher than in the synthetic system.

The Li concentration in albite is plotted against Li in chlorite in figure III-7. Only 65 percent ($r^2 = 0.65$) of the Li variation in albite is explained by a linear variation with Li in chlorite. The regression line has a slope of 2.39 ± 1.51 and an albite intercept of -228 ± 237. Points 53, 54, 56, and 58 make a much better line($r^2 = 0.97$) with a slope of 0.99 ± 0.27 and an albite intercept of -88 ± 36. It is not clear whether the distribution curve in this experiment is linear at low concentration (points 53, 54, 56, 58) and then curves through 57, 59, and 65, or whether a single regression line should go through all the points. If all the points are considered the origin is within the error limits of the intercept. The error limits of the average $D^{alb-chl}$ (0.81 ± 0.64) overlap with the error of the slope of this regression line.

In summary, a significant difference between $D^{alb-chl}$ of the natural and synthetic systems was not resolved. There were not enough data points for the natural minerals to establish a meaningful curve for

an albite-chlorite Li distribution. Therefore, the average $D^{alb-chl}$ will have to serve as the best estimator of Li paritioning between natural chlorite and albite.

Before the Li distribution measured in this study can be widely used, the effect of solution composition should be assessed. In figure III-8 individual lithium partition coefficients are plotted against ionic strength of the vapor phase. No covariation between $D^{alb-chl}$ and ionic strength is evident. Ionic strength may influence lithium partitioning if adsorption plays an important role in Li uptake in the minerals. If equilibrium was established between the vapor and the interior of each mineral so that Li partitioning was controlled only by crystal structure then the $D^{alb-chl}$ should be independant of solution composition unless the mineral was changed by this composition. The vapor should only communicate the chemical potential of Li in albite with that of Li in chlorite.

III-3 Analytical uncertainty and variation of lithium distribution

An important question to resolve is whether or not the variation in $D^{alb-chl}$ is due to analytical uncertainty or to failure in achieving equilibrium and to other experimental error. If the error in the average $D^{alb-chl}$ value is less than or equal to that predicted from the analytical uncertainty, then one could argue that the reported error in the partition coefficient is chiefly analytical. If the observed error is greater than the predicted analytical error then there is a good possibility that the reaction did not reach equilibrium in some

Figure III-8 Lithium partition coefficients between albite and chlorite at 500^0 C. (+) and 600^0 C. (O) plotted against the ionic strength of the vapor.
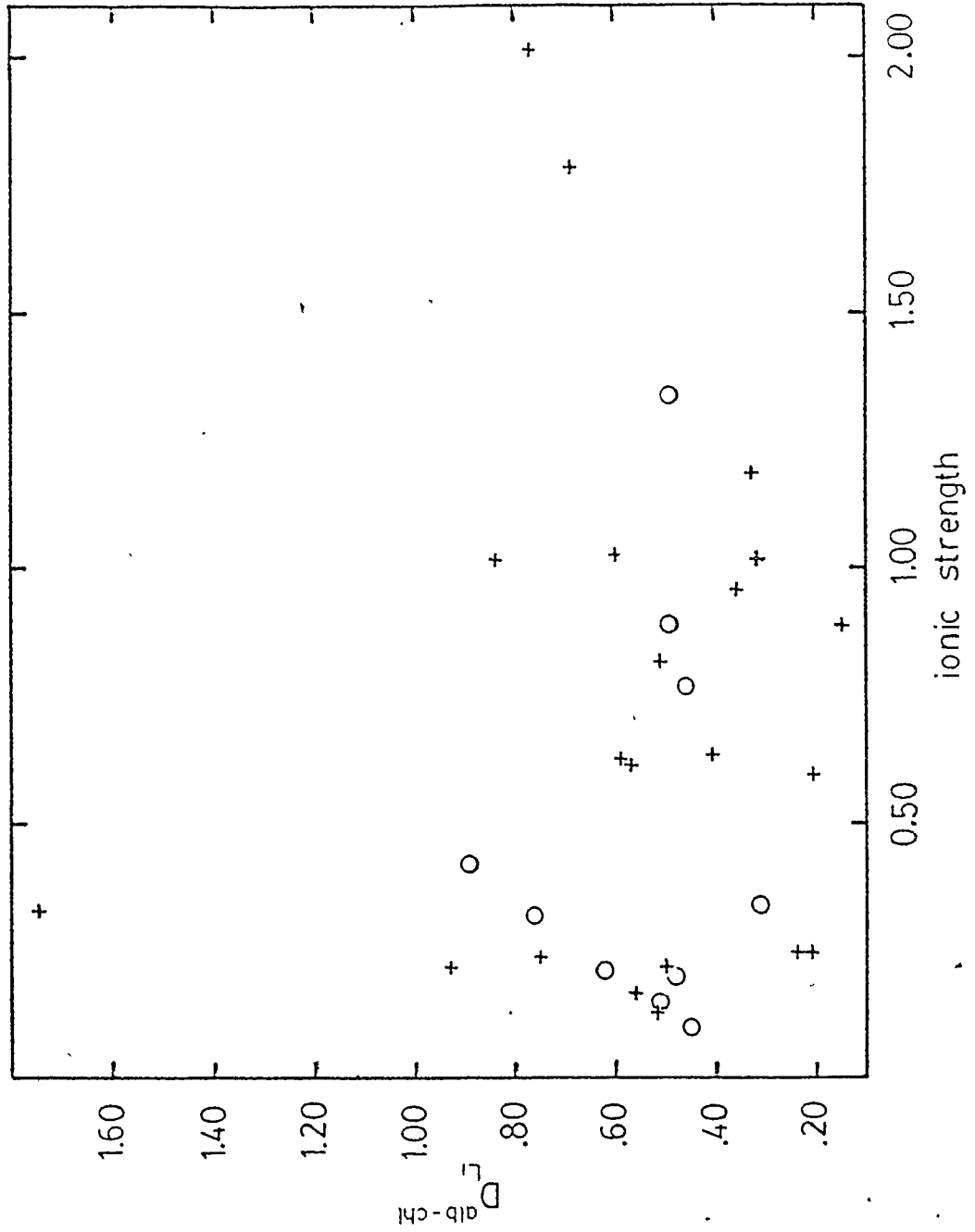
cases.

The standard deviation of the average $D^{alb-chl}$ shown in table III-4 represents a 41 percent error. However, if the error of the mean at the 90 percent confidence level is used (table III-4) the error is only 11 percent. This is a better estimator of the error in the combined data, while the standard deviation represents the expected error in a single measurement. If the slope of the regression line in figure III-7 is used to estimate $D^{alb-chl}$ the error is 13 percent.

Estimated analytical errors are given for each Li concentration in table A-5. Since partition coefficients are calculated from two Li concentrations, the errors of these Li concentrations must be combined to obtain the error for the partition coefficient. If the Li concentration in albite is A ± a and the Li concentration in chlorite is B ± b then the partition coefficient is given by:

(1) $$D^{alb-chl} = (A \pm a)/(B \pm b)$$

(2) $$A/B(1 \pm a/A)(1 \pm b/B)^{-1}$$

If $b/B << 1$ then the binomial theorem gives:

(3) $$(1 \pm b/B)^{-1} = 1 \pm b/B \text{ plus smaller terms}$$

Substituting (3) into (2) one gets:

$$D^{alb-chl} = A/B(1 \pm a/A \pm b/B \pm \text{ smaller terms})$$

(4) $$A/B \pm (a/b \pm bA/B^2)$$

Equation (4) gives the absolute error of the partition coefficient. However, the relative error is in a less awkward form and

is given by:

$$(a/\beta + bA/\beta^2) \times (B/A) = a/A + b/\beta$$

Therefore, the relative error of the partition coefficient is given by the sum of the relative errors of Li in albite and chlorite. The relative analytical error of each $D^{alb-chl}$ is given in table III-3. These analytical uncertainties ranged from 6 to 116 percent, with a mean of 32 percent. The observed standard deviation of $D^{alb-chl}$ was higher than the average predicted analytical uncertainty. In the experiments with Mg-chlorite 6 out of 43 samples exceeded the standard deviation of the mean $D^{alb-chl}$ by more than could be accounted for by analytical uncertainty. This suggests that experimental error and/or lack of equilibrium may have affected some samples.

III-3 Location of lithium in the mineral phases

Knowing the location of Li in the mineral phases is essential to the full understanding of lithium distribution coefficients. Lithium could be located in lattice sites, in defect structures, or it could be adsorbed onto mineral surfaces. In this study it was impossible to differentiate between the first two possibilities. It is hoped that adsorbed Li was removed by boiling the minerals in a 10^{-2} N HCl solution for 15 minutes. The adsorbed Li would be removed by the effect of high temperature and by exchanging with the hydrogen ion. The hydrogen ion concentration in this solution corresponds to the pH at which albite and SiO_2 suspensions lose their negative charge (zero point of charge), (Stumm and Morgan, 1970).

Assuming that Li is not adsorbed or located in crystal defects, the lattice sites occupied by Li are still not very clear. In feldspar Li should favor the M site, usually occupied by Na, K, or Ca, because of valence (Smith, 1974). However, Li is considerably smaller than K or Na, making substitution with these elements difficult. The shorter Li-O bonds would tend to deform the crystal structure. Volfinger (1970), Iiyama (1974b) and Iiyama and Volfinger (1976) have produced a model which relates element partition coefficients to local crystal deformations produced by these elements.

In chlorite Li has been assumed to substitute for Mg in the octahedral sites in the talc layer or in the brucite layer. To maintain charge balance Si must substitute for Al in the tetrahedral sheet or Al substitutes for Mg, possibly in the brucite layer. Robert and Volfinger (1979) showed that Li was located in the octahedral position in lepidolite. On the other hand Volfinger and Robert (1979) indicated that in phlogopite Li does not substitute for Mg in the octahedral position, but instead enters the tetrahedral sheet. Evidence for this includes a lack of correlation between Li content in phlogopite and Mg concentration in the vapor. In lepidolite d_{060} decreases with increasing Li because Li replacing Mg in the octahedral position distorts the sheets. In phlogopite d_{060} does not decrease with increased Li content. The d_{005} decreases sharply with Li in phlogopite, suggesting that Li enters the interlayer sheet causing the interlayer distance to decrease. The authors also state that Li cannot substitute into the alcalin site, inside the tetrahedral sheet, because of Li's small size. They propose that Li

enters the base of those tetrahedra, in which Al^{+3} has replaced Si^{+4}.

Chlorite structure differs from phlogopite in that the octahedral

layer is sandwiched between single layers of tetrahedra, instead of

double layers as in phlogopite. Perhaps in chlorite Li could also

be located in the bases of tetrahedra which contain Al. In chlorite the

bases of these tetrahedra face the brucite layer. This would be an

alternate location of lithium to the commonly assumed octahedral position.

The range in lithium concentration was too small to determine

structural changes in chlorite due to Li uptake.

In summary, if Li does not enter defect structures, then

it may substitute into the K sites in albite. In chlorite it may

replace Mg in the talc or brucite layer or it may be lodged in the

base of tetrahedra containing aluminum.

CHAPTER IV

CONCLUSIONS

IV-1 Statement on measured Li distributions

In this study Li distributions appears to be insensitive to temperature in the range 400^0 to 700^0 C. The effect of ionic strength was also not measurable over the range of ionic strengths of 0.1 to 2.0. Lithium prefers to enter chlorite on a 2:1 weight ratio ($D^{alb-chl}$ = 0.56 ± .06). In the system with Fe-chlorite and natural albite there is a slightly higher, but not significant preference for albite ($D^{alb-chl}$ = 0.81 ± 0.40). In the synthetic system Li distribution between chlorite and albite seems to obey Henry's law up to at least 600 ppm Li in chlorite. In the natural system the Li distribution plot between albite and chlorite did not give a clear enough curve to say whether or not Henry's law was obeyed.

There is considerable doubt as to the accuracy of vapor-mineral distribution measured in this study because of the poor Li mass balance. However, the range of these Li distributions may be obtained from table A-10 in the appendix. Lithium appears to favor the vapor phase over both albite and chlorite..

IV-2 Comparison to published Li distributions

Lithium distribution between albite and chlorite in a common vapor phase has not been measured before this study. However, if sanidine can be considered as a feldspar analogue to albite, and if muscovite and phlogopite are sheet silicate analogues to chlorite then a comparison can be made between the literature and $D^{alb-chl}$ in this study. Lithium distribution between vapor and sanidine and muscovite at 600^0 C and 1 kb was measured by Volfinger (1970). Volfinger and Robert (1979) measured Li exchange between vapor and phlogopite under the same conditions. It is difficult to directly compare these Li distributions with this study because they were presented as Li/K ratios. The variation of these Li distributions with solution composition is shown in figure IV-1. The vapor-mineral distributions in figure IV-1 can be combined to obtain feldspar-sheet silicate Li distributions shown in table IV-1.

Table IV-1

$\log_{10}(Li/K)_{aq}$	$K_{D\ Li-K}^{san-musc}$	$K_{D\ Li-K}^{san-phlog}$
-3	6.31	0.89
-2	0.59	0.45
-1	0.25	0.45
0	0.56	0.71

The exchange coefficients shown in table IV-1 vary with the Li/K ratio in solution, but are not very different from the $D^{alb-chl}$ in this study. A notable exception is the Li exchange between sanidine

Figure IV-1 Li/K distribution coefficients between vapor and minerals plotted against the Li/K ratio in the vapor at 600^{0} C and 1.0 kb. Ratios are in atomic numbers. (Volfinger, 1970: Volfinger and Robert, 1979)
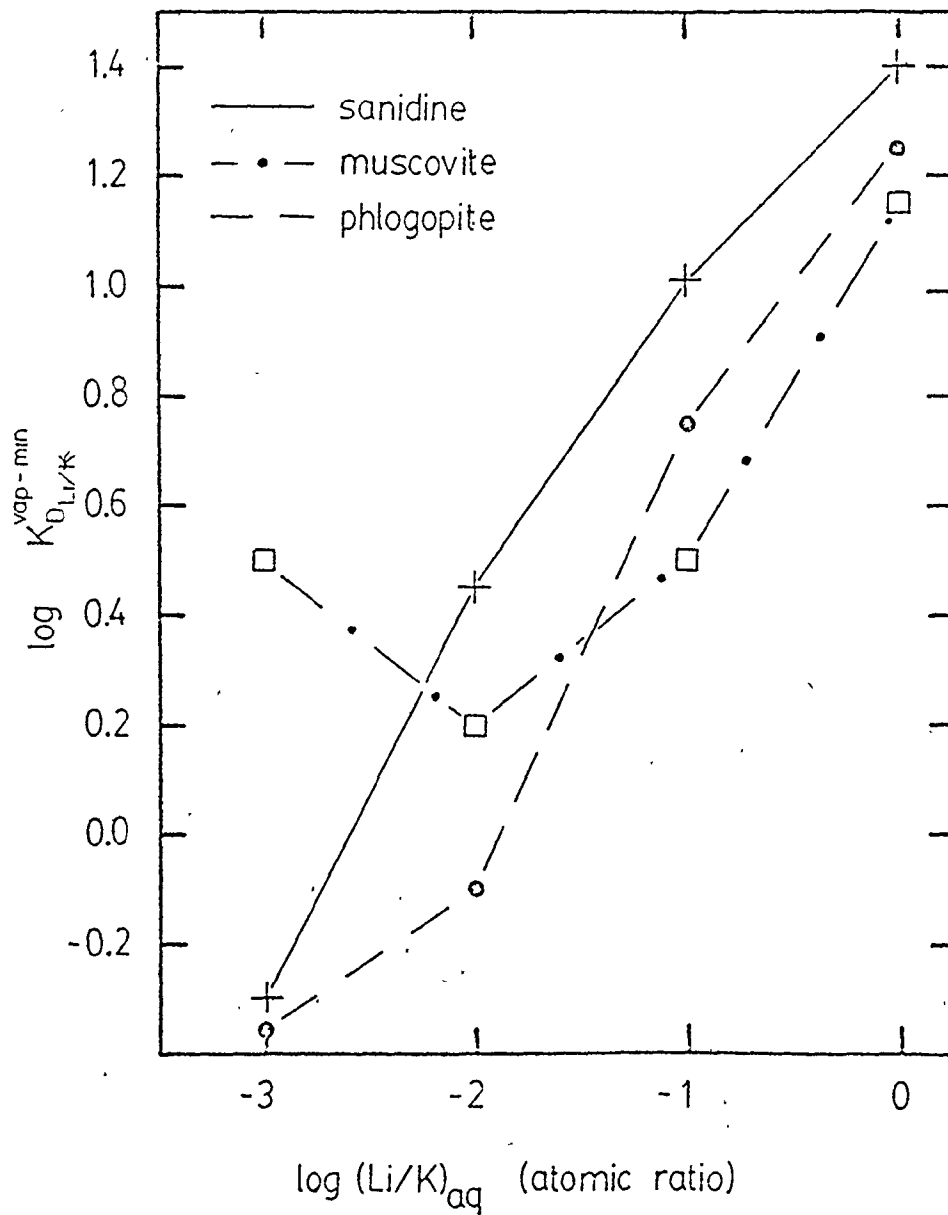
and muscovite at a Li/K ratio of 10^{-3}, where Li prefers to enter the feldspar.

IV-3 Comparison to Li concentration in natural albite and chlorite

Smith (1974) summarizes lithium concentrations in feldspars. In general feldspars contain 0 to several 10's of ppm Li. Highest concentrations of Li are found in pegmatites. Gordienko and Komenstev (1969) reported Li concentrations in microclines ranging from trace to 2,200 ppm, with most values being between 90 and 500 ppm. There was only one sample with 2,200 ppm Li and the possibility exists that this microcline could have been contaminated with mica or spodumene. In this study Li concentrations in albite ranged from 2 to 574 ppm. Compared to average feldspars this is rather high. However, if alkali feldspars in some pegmatites actually do contain high Li concentrations, then the Li content of albite in this study is not unreasonable.

Neiva (1980) reported Li values in chlorites and biotites in metasediments intruded by a granite. The background concentration of Li in a green phyllite was 260 ppm. At the granite contact chlorite contained 300 ppm Li in the phyllite and 533 in the hornfels. In the aplite pegmatite and in quartz veins chlorite contained 358 and 347 ppm Li. The chlorite from Whitefish Falls, used in this study, contained 75 ppm Li before the experiment. In this study the Li content of synthetic chlorite ranged from 37 to 664 ppm. Therefore, the experimental Li concentrations in chlorite can be found in nature, and do not represent unusually high levels.

As was pointed out in the introduction, most of the lithium in spilites appears to be contained in chlorite. Albite seems to be virtually free of lithium. The results of this study strongly contradict the apparent Li distribution in spilites.

To determine whether or not the estimated range of Li distribution between vapor and chlorite can explain Li concentration in spilite a Li mass balance calculation was undertaken. For this calculation the lowest $D^{vap-chl}$ value was used since this removes Li from the vapor most efficiently. (See appendix A-6)

given; - $D^{vap-chl} = 1.10 \pm 0.60$ (table A-10)

- an average spilite with 75 ppm Li (Shaw et. al., 1977)

- Assume that chlorite accounts for 100 % Li.

- (1) If 10 % chlorite then chlorite contains 750 ppm Li.

- (2) If 20 % chlorite then chlorite contains 325 ppm Li.

then: - Chlorite (1) equilibrates with a solution of 825 ppm (range: 375 to 1275 ppm)

- Chlorite (2) equilibrates with a solution of 412 ppm (range: 187 to 637 ppm)

To account for the hypothetical Li concentrations in chlorite the amount of Li required in the vapor can be rather high, particularly if the higher $D^{vap-chl}$ value is more correct. Shaw et. al. (1977) summarized Li concentrations in some natural waters. General hydrothermal waters contain 8.2 ppm Li. Subsurface brine at Niland Well, Imperial Valley, Calif. contains 321 ppm Li. It is possible that the 412 ppm Li

vapor concentration called for in case 2 may exist in nature. However, if general hydrothermal waters contain only 8 ppm Li then a special case seems to be called for to get 412 ppm Li in a natural vapor. If the lower range of $D^{vap-chl}$ is correct then the average chlorite will lose Li to the average hydrothermal water.

In summary, Li distributions between vapor, albite, and chlorite at 400^0 C to 700^0 C do not explain Li distribution in spilites very well. To obtain Li enrichment in spilites anamolously high vapor Li concentrations are called for or the partitioning of Li into chlorite must be more efficient. These more efficient distribution coefficients may exist at temperatures below 400^0 C.

IV- 4 Alternate mechanisms of Li enrichment in spilites:

To explain the low concentration of Li in albite compared to chlorite in natural spilites a non-equilibrium situation could be called upon. However, this is probably not necessary since the vapor-mineral distributions at 400^0 C seem to be too high to allow concentration in the solid phases.

The concentration of Li in spilites may take place at lower temperatures (below 300^0 C). Ellis and Mahon (1964) found that the maximum Li leached in hot-water-rock reactions was a direct function of temperature. Thompson et. al. (1972) and Thompson (1973) showed that Li is enriched during the low temperature alteration of basalt. Considering the amount of Li enrichment which is required for chlorite, and assuming that the average hydrothermal water only contains 8 ppm Li, the water-mineral distribution coefficients should be much less than

unity (preferably 0.10 to 0.01). Such a situation can exist in the sedimentary enviroment where Li is precipitated in certain clay minerals, manganese oxides, and phosphates.

Basalts could be spilitized during greenschist metamorphism without Li enrichment. After the rocks have cooled, low temperature brines, formation waters or ground waters would pass through the rock. Lithium from these waters would be adsorbed by chlorite or clays and oxides closely associated with chlorite. The more highly altered basalts would contain more chlorite and therefore would have a higher cation exchange capacity. This might account for a positive correlation between Li concentration and the degree of alteration. An analogy to this would be the concentration of Li in clay-rich sediments relative to those with little clay.

Another mechanism of Li enrichment could be concentration from a very Li rich brine. The aqueous phase could be lost to mineral hydration or it could be periodically boiled away. Lithium would be precipitated because of super-saturation. The problem with this scenario is that it calls for a special case. It may not be applicable as a general rule.

APPENDIX

A-1   Experimental proceedure

This section describes the experimental synthesis of chlorite and albite in equilibrium with a Li containing vapor.   Preparation of experimental products for Li analysis is also described.

The gold tubing used in the experiments was supplied by Johnson Matthey and Mallory Limited.   Before use the gold was boiled in 6 N HCl to remove contamination and eliminate impurities which may interfere with welding.   The size of the gold tubing used is given in table A-1.

Table A-1

Gold tubing and pressure vessels

		inner diameter	outer diameter	length
gold (A)	main capsule	0.10 inches	0.12 inches	1.5 inches
tubing (B)	inner capsule	0.05 "	0.07 "	0.75 "
pressure	112 R	0.50 "	2.0 "	10.5 "
vessels	114 R	0.25 "	1.0 "	9.25 "

The amount of each mineral gel used in the experiments varied from 10 to 20 mg.   The chlorite gel was first weighed into the smaller capsule, B.   The ends of this capsule were crimped just enough to prevent the escape of the gel, but not enough to prevent the vapor

phase from communicating with the contents. After one end of the main capsule was welded with a carbon D. C. arc welder, capsule B was placed in A along with the albite gel. The solution (8 to 36 mg) was introduced by means of a syringe. After weighing, capsule A was crimped shut and welded. To prevent the solution from boiling away the capsule was held in an ice bath during the welding proceedure.

The weight loss during welding was checked. Usually the weight loss was under 1 mg and could be accounted for by gold volatilization. The samples were left overnight at 110^0 C and then checked for leaks. Samples with leaks were discarded.

The samples with Fe-chlorite were treated in a similar way except that a Ni-NiO buffer also had to be used to control oxygen fugacity. The albite and chlorite were each weighed into a B-type capsule, and both were crimped and placed into the A-capsule. The powdered Ni-NiO buffer (20 to 30 mg) and the solution (30 to 60 mg) were added, then the capsule was welded in the usual manner. After the experiment the buffer was checked with X-ray diffraction to see if both Ni and NiO were still present.

The pressure vessels used were the cold seal, Tuttle type, made of Rene 41 alloy. They were supplied by Leco, Tem-Pres Division. See table A-1 for dimensions. Hydraulic pressure was delivered to the pressure vessels by a piston type, air-operated, boost pump. The pump was manufactured by Teledyne Sprague Engineering. Pressure gauges were made by American Instrument Co. Inc. Once the samples had reached the desired temperature and pressure the variation in pressure was believed

to be less than 1,100 psi (0.08 kb).

The pressure vessels are heated by external furnaces, whose temperatures were controlled by Fisher pyrometer controllers (13-917). The sample temperature was monitored by chromel-alumel thermocouples mounted in the pressure vessel, close to the sample. The temperature reading was given by the Speedomax W multipoint controller. Temperature variation during equilibration was believed to be less than 10^0 C. The accuracy of the recorder in conjunction with the thermocouples was standardized with the melting temperature of NaCl (800^0 C).

The gold capsules were placed in the pressure vessels along with a filler rod which reduced the amount of water in the vessel. This helped to reduce temperature variations due to convection and minimized the danger of explosion in case the vessel failed under pressure. The small vessels can hold two gold capsules, while the larger bombs may hold four. Over-loading causes capsules to stick together.

After completion of the experiment the bombs were cooled by an air stream. After fifteen minutes the vessels were cool enough to immerse in water. During the quenching pressure was maintained until the vessel was ready to be opened. The gold capsules were removed from the bombs and weighed to check for leaks. In some cases weight differences could be attributed to other factors besides leaks. For instance, gold capsules were stuck to each other and exchanged gold upon separation. Certain capsules appeared to have corroded slightly and may have lost some gold.

Each gold capsule was then submerged in a minimum amount of deionized water and pierced. After bubbling had ceased the capsule was opened with scissors and a knife. The minerals were separated and boiled initially for ten minutes to remove adsorbed Li. The minerals were separated from the solution by filtration through a millipore system. Millipore and Whatman filters were used. The gold scraps were also boiled to remove adsorbed Li. All the washings were combined and reduced to 10 to 20 gm by evaporation, and then acidified with HNO_3 for future analysis. The first Li analysis of minerals showed irregular results, suggesting that Li was still adsorbed onto the mineral surfaces and that in some cases the samples were spread too thinly on the filter paper during the activation analysis. Therfore, the minerals were boiled again in a 10^{-2} N HCl solution to further remove adsorbed Li. Before activation analysis the minerals were concentrated in a smaller area on the filter paper to insure an even distribution.

The minerals were X-rayed while still on the filter paper. Often the small amount of sample produced a poor diffractogram. Small amounts of sample were also used to make grain mounts for optical examination. Optical microscopy was more useful with the natural samples, where the albite and chlorite could be clearly destinguished. The synthetic products were very fine-grained. The colorless nature of clinochlore made its identification more difficult.

A-2 Preparation of gels and Li-standard gels

Gels of albite and clinochlore composition were prepared in a similar way to the method of Luth and Ingamells (1965). Sources of the element oxides used in the gel manufacture are given in table A-2, along with the gel compositions.

Table A-2

oxide	source
SiO_2	tetra-ethyl orthosilicate $(C_2H_5O)_4Si$
Al_2O_3	Al metal
MgO	MgO
Na_2O	Na_2CO_3

albite gel: $0.5\ Na_2O \cdot 0.5\ Al_2O_3 \cdot 3\ SiO_2$

chlorite gel: $5\ MgO \cdot Al_2O_3 \cdot 3\ SiO_2$

chlorite-albite gel: $(5\ MgO \cdot Al_2O_3 \cdot 3\ SiO_2) + (0.5\ Na_2O$

$$0.5\ Al_2O_3 \cdot 3\ SiO_2)$$

$$= 5\ MgO \cdot 1.5\ Al_2O_3 \cdot 0.5\ Na_2O \cdot 6\ SiO_2$$
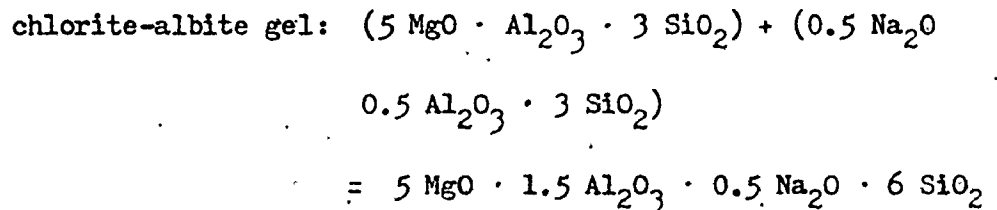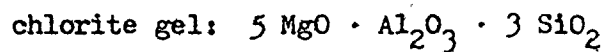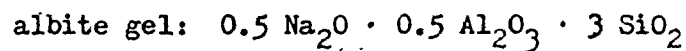
To make the gels Al, MgO, and Na_2CO_3 were weighed into a teflon beaker and dissolved with a minimum of 6 N nitric acid, over a water bath. After dissolution was complete the solution was allowed to evaporate to near dryness. A small amount of 25 wt % ethanol was added to dissolve all crystals. The required amount of tetra-ethyl ortho-silicate (TEOS) was weighed into a plastic weighing bottle. The bottle was kept covered as much as possible to avoid evaporation. The TEOS was washed into the teflon beaker with the ethanol solution. A minimum

amount of ammonium hydroxide was added until the solution became a gel.

The product was left overnight to allow complete gelling, and then was heated in a furnace at 110^0 C to remove excess ammonium hydroxide. The contents of the beaker were ground in an agate mortar and pestle and transferred to a platinum crucible. This was heated over a burner until most of the nitrates were decomposed. To ensure complete decomposition, the gel was left overnight in a muffle furnace at 700^0 C. The product was again ground in an agate mortar and pestle. Since this product is an amorphous solid which shows no X-ray diffraction pattern and no birefringent material it is refered to as a gel.

The Li standards used in the irradiation analysis were made in a similar way, and had the basic composition of clinochlore. A known amount of a 1000 ppm Li solution was added to the teflon beaker after the Al, Na and Mg had dissolved. The expected Li concentration was calculated using the μg Li added and the final yield of the gel in grams. In this calculation Li loss during gel manufacture was accounted for by determining the percent weight loss of material during grinding and transferring, and then reducing the amount of Li by this percentage. A comparison of expected concentration and analysed Li concentration is given in table G-2. Differences in these values could be due to errors in the calculation of expected Li concentration. The analysed Li values were used in this study.

Table A-3

Li-gel standards

gel	expected ppm Li	analysed ppm Li
CHL-1	140	139
CHL-2	247	277
CHL-3	593	576
CHL-4	637	655
CHL-5	1179	1194
CHL-6	41	6
"Li chlorite"	1065	992

A-3 Procedures with atomic absorption

In this study atomic absorption was used for the analysis of (1) the Li-gel standards, (2) the experimental vapor phase, and (3) the natural minerals containing boron. Since the procedures used in the above three cases were slightly different, they will be described separately.

To analyse the Li-gel standards 100 to 500 mg of sample were weighed into a teflon beaker, then dissolved in 12 ml of an acid mixture $(HF + HClO_4 : 3/1 : v/v)$ and 1 ml of HNO_3. When dissolution was complete the solution was allowed to evaporate over a sand-bath. The residue was washed into a beaker and 5 ml of $HClO_4$ plus water (1:1) was added. The solution was boiled to dissolve all salts. After transfering to a plastic bottle the solution was diluted to 100 gm. The standards contained the same amount of $HClO_4$ as the samples. The standard matrix contained the same amount of Mg and Al as would be expected in the sample

solution. The Li analyses were compared to the international standard
reference samples Basalt BR, Basalt BM, and Slate TB. See the section
on errors and table II-1.

The vapor samples were acidified with 6 to 10 drops of 6 N
HNO_3 and stored in 30 ml plastic bottles. The amount of solution in the
bottle was determined by weight. A Li standard in a 1 % nitric acid
matrix was used to measure Li. The major cations were determined with
a Al, Na and Mg standard in a 1 % nitric acid matrix.

In the analysis of the natural minerals 1 to 20 mg of sample
were weighed into a teflon crucible. The sample was decomposed with 10
ml HF and 1 ml $HClO_4$. After dissolution and evaporation of HF and $HClO_4$
the sample was dissolved with 10 ml of 1 N HCl. Perchloric acid was
not used in the final solution since it was expected that some samples
would have to be analysed with the graphite furnace, and $HClO_4$ attacks
the graphite tube. The solutions were transferred to plastic bottles.
The final solution weight was reduced to between 7 and 30 grams. Li
analysis was carried out using a Li standard in a 4 % HCl matrix. The
graphite furnace had to be used when solution composition dropped to
.015 ppm Li.

A-4 Alpha track Li analysis

This method takes advantage of the reaction ^6Li (n,α) ^3H. It is assumed that ^6Li has a constant isotopic abundance of 7.5 atom percent. It is also assumed that during irradiation with neutrons, the number of alpha particles produced is directly proportional to the number of Li atoms present in the sample. The alpha particles are recorded on a cellulose nitrate film. After etching, the alpha tracks are counted to determine the amount of Li present.

The sample must be free of interfering elements which also emit alpha particles. The main interference comes from boron because of the following reaction: ^{10}B (n,α) ^7Li. The neutron cross-section for the boron reaction (3,837 barns) is much larger than for Li (940 barns). Therefore, the presence of small amounts of boron may mask the alphas emitted by Li. Owing to the presence of some boron in most natural materials this analytical technique is limited to boron-free systems. Since the alpha track method is rather time consuming it is not very useful for general Li analysis except under special circumstances.

In this study the alpha track method did have some advantages over atomic absorption. This method is nondestructive so that the sample can be saved for further study. The sample mass is also very small, so when samples are dissolved for A.A.S. the concentration of Li may become too dilute to analyse. This method could detect 6 ppm in the sample where as A.A.S. might only detect 30 ppm, depending on the sample size. If the grain size of the synthetic minerals had been larger the alpha track method may have showed whether or not Li was evenly distributed in each grain. However, some samples showed occasional high

density patches of alpha tracks which seemed to radiate from a single point source. This point source could have contained an anomalous Li amount due to the presence of a Li salt or it may have represented contamination from an interfering element such as boron. Since the track density of these spots was greatly different from the over all density of the sample the high density patches were not counted. If these high density patches did represent a precipitated Li salt the atomic absorption method would not be able to distinguish this contamination. Consequently with A.A.S. the mineral's Li concentration would be too high.

During the irradiation the synthetic minerals were left on the filter paper. The filter paper was taped to a cardboard backing (2.5 × 3.5 cm) which had been wrapped with C-39 plastic polyethylene to screen any alphas from the cardboard. The advantage of cardboard over plexiglass slides is its low cost and smaller thickness. This allows one to irradiate more samples at once. The powdered minerals were spread as evenly as possible on the filter paper. Variations in alpha track density could be produced if the sample surface is not even and all areas of the film are not in direct contact with the sample. Alpha particles are easily blocked so that the activity recorded on the film may only be from a thin surface layer. Therefore, the total thickness of the sample may not be important. A small piece of cellulose nitrate CA 80-15 film is taped over the sample area. The cellulose nitrate film is damaged by alpha particles emitted from the sample. The sample is then wrapped with plastic polyethylene, which prevents stray alpha particles from entering or leaving the sample. After etching, the alpha tracks in

the film are revealed. The film was manufactured by Eastman Kodak.

Up to about 20 samples were wrapped together to make a single package. The Li-gel standards were evenly interspaced throughout each sample package, so as to reduce the effect of any point-to-point variation in the neutron flux. Each sample package included a set of standards.

The samples were irradiated in the McMaster reactor. The sample packages were suspended in RIFLS 9E, 23 cm below the lid. The samples were rotated to insure an even distribution of neutron flux. At this position the slow-neutron flux was about 5×10^{11} neutrons/sec. The exposure time was about one minute. After two days the sample radioactivity (0.1 to o.5 M.R./hr.) was low enough for easy handling.

The samples were cut open and the cellulose nitrate film was washed to remove all traces of the sample. The films were etched in 2.5 N NaOH for 25 minutes at 60^0 C. After development the films were washed and allowed to dry.

The films were mounted on glass slides so that they could be photographed on Kodak Plus-X or Tri-X film through a petrographic microscope. Two frames were taken of each sample. The area of the cellulose nitrate film covered by each photograph was 13.76 mm^2. Using a film-strip projector the negatives were projected on a wall onto a target grid divided into 14 areas. The alpha tracks in each of $(14 \times 2 = 28)$ areas were counted for each sample. The area of the cellulose nitrate film represented by each area was usually 1.0 mm^2. In some groups (M,N,Q), where the track density was very high, the size of each area was reduced to $\frac{1}{2}$ or $\frac{1}{4}$ mm^2.

For each sample the alpha counts were averaged and a standard deviation was calculated. To eliminate the effect of spurious data all counts which differed from the mean by more than one standard deviation were dropped and new means and standard deviations were calculated. Spurious counts could have been produced by an uneven sample surface, local contamination or difficulties·in counting when parts of the photographed surface were slightly out of focus. Anamalously high or low values could have produced skewed populations. When data points exceeding one standard deviation are dropped, the remaining alpha counts may approach a more normal distribution. In most cases the average alpha counts for a particular sample did not change by more than two counts, which was less than the standard error of the mean.

The average alpha counts of Li standards from selected groups are plotted against ppm Li in figure A-1. These alpha counts, along with calibration line regression coefficients for each sample group are shown in table A- 4. The considerable differences in alpha counts between the sample groups result from variations in exposure time and height of sample in the RIFLS tube. Due to these variations it is necessary to use a set of standards in each sample package. The calibration curves appear to be linear since usually more than 88 % (r^2 = 0.88) of the variation in alpha counts is accounted for by a linear relationship with ppm Li.

Table A-5 gives the alpha counts and calculated Li concentrations for each sample. The reported errors were given by the 90 % confidence interval of the mean. The Li concentration for a sample

Figure A-1 Selected calibration curves relating alpha counts per area to ppm Li. Error bars represent the 90 % confidence interval of the mean alpha counts for each standard. Dashed lines represent the 90 % confidence interval of the mean response. Differences in the calibration lines result from variations in exposure time and hieght of samples in the RIFLS tube.
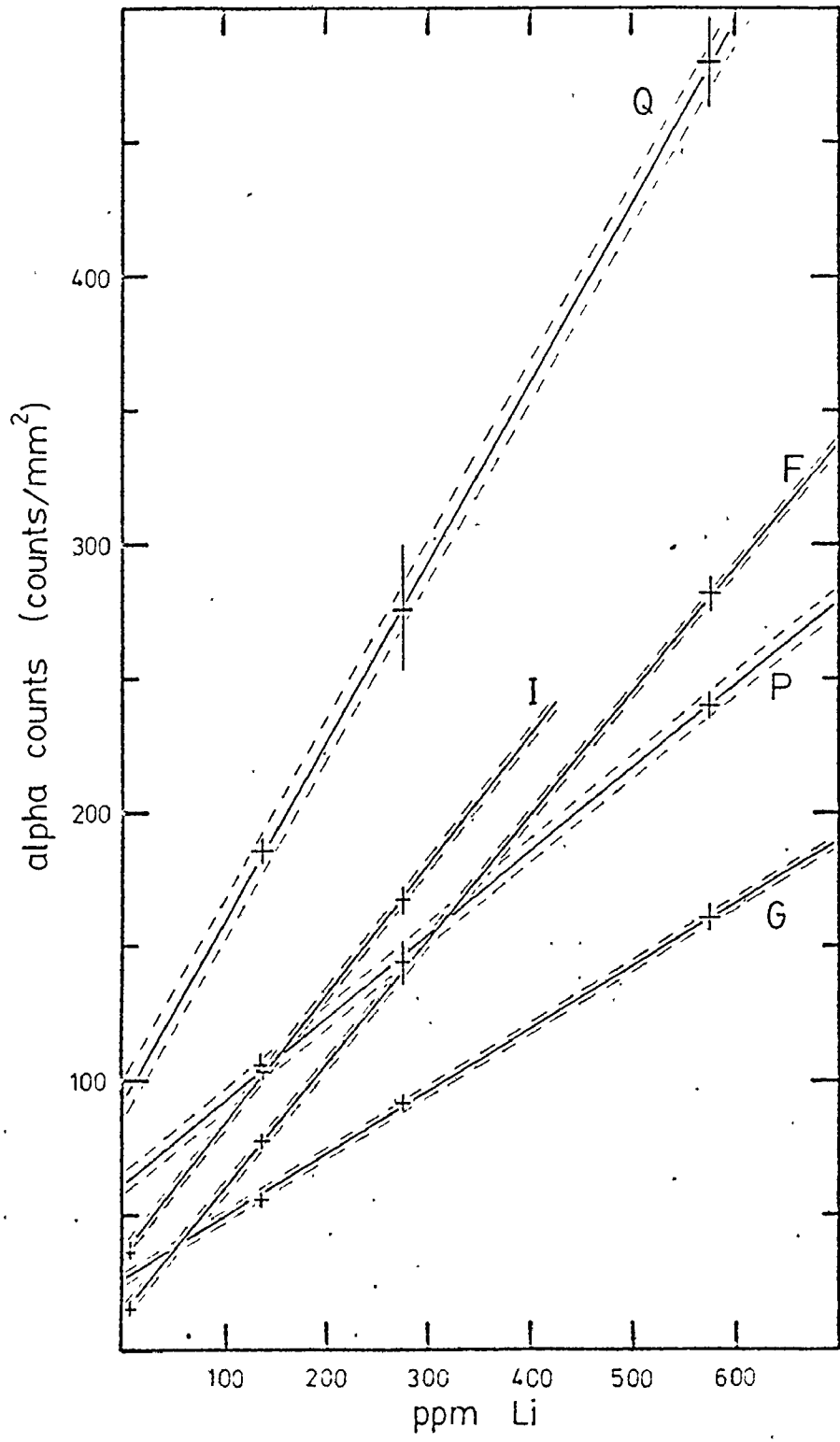
Table A- 4

Alpha counts of Li standards and calibration line regression coefficients

sample group	a_0	a_1	r^2	CHL-6	CHL-1	CHL-2	CHL-3
F	11.96	0.4662	0.99	15.3 ± 1	78.8 ± 2		281 ± 6
G	24.98	0.2369	0.96		58.3 ± 2	92 ± 3	161 ± 5
I	34.32	0.4869	0.97	36.4 ± 3	104 ± 3	168 ± 5	
* M	57.38	0.2243	0.97	208 ± 9	370 ± 7	494 ± 14	738 ± 15
* N	122.24	0.1544	0.88		566 ± 13	674 ± 8	841 ± 19
# O	169.47	0.3482	0.94	346 ± 12	438 ± 15		739 ± 31
P	60.91	0.3091	0.90		106 ± 5	144 ± 8	240 ± 5
Q	91.22	0.6725	0.98		186 ± 5	276 ± 30	480 ± 17
ppm Li in standards				6	139	277	576

* Regression coefficients are based on areas of $\frac{1}{4}$ mm^2.

\# Regression coefficients are based on areas of $\frac{1}{2}$ mm^2.

Errors in alpha counts are the 90 % confidence interval of the mean given by: $t_{\alpha/2} (S/\sqrt{n})$

The coefficient of determination, which gives the fraction of the variation in alpha counts which is accounted for by a linear variation with ppm Li, is given by:

$$r^2 = (\Sigma XY - (\Sigma X \Sigma Y))^2 / ((\Sigma X^2 - (\Sigma X)^2/n) (\Sigma Y^2 - (\Sigma Y)^2/n))$$

where: X = ppm Li   Y = alpha counts per area

Equation of the calibration line: counts = a_0 + a_1 ppm Li

Table A-5

Alpha counts per area and Li concentrations

sample group	sample number	counts in albite		counts in chlorite		ppm Li in albite		ppm Li in chlorite	
* M	1	129	± 5	186	± 4	319 ± 22		571 ± 18	
I	3	74.7	6	112	3	83	12	159	6
* M	4	72.4	3	82.6	3	67	13	112	13
* M	5	81.4	3	92.5	3	107	13	156	13
* M	6	129	5	203	5	319	22	648	22
P	7	98.5	3	110	5	122	10	158	16
* M	8	126	3	206	3	304	13	664	13
* M	10	186	5	178	6	574	22	538	27
P	11	71.5	4	74.7	4	34	13	45	13
* N	12	135	4	148	5	80	26	164	32
* N	13	131	3	142	6	60	19	126	39
* N	14	144	3	132	4	122	19	138	26
* N	15	156	2	164	3	222	13	267	19
P	16	67.4	3	80.0	8	21	10	62	26
I	19	67.1	5	136	8	67	10	209	16
* N	20	135	4	137	4	83	26	93	26
G	21	59.0	4	107	5	143	17	348	21
I	24	155	9	178	10	248	18	295	21
* N	25	128	3	155	5	35	19	78	32
P	26	129	6	152	7	221	19	295	23
P	27	76.6	5	98.0	3	55	16	120	10
* N	28	157	3	159	4	222	19	238	26
P	29	65.55	3	72.3	3	15	10	37	10
P	30	72.3	4	83.1	6	37	13	72	19
# O	31	181	4	190	6	34	11	60	17
Q	32	111	3	135	4	30	4	65	6
# O	33	178	5	184	7	42	14	24	20
Q	34	140	5	194	11	73	7	153	16

Table A-5 continued

sample group	sample number	counts in albite		counts in chlorite		ppm Li in albite		ppm Li in chlorite	
F	35	60.4 ±	4	191 ±	15	104 ±	9	383 ±	32
# O	36	198	7	263	7	83	20	268	20
Q	37	117	4	209	7	39	6	175	10
Q	38	185	8	279	11	140	12	279	16
Q	39	110	5	183	5	28	7	136	7
# O	40	189	4	249	7	56	11	229	20
# O	41	188	5	205	16	52	14	102	46
Q	42	113	2	152	6	32	3	90	9
F	43	28.9	5	92.7	10	36	11	173	21
# O	46	209	6	249	8	112	17	227	23
Q	47	131	3	211	6	59	4	178	9
# O	48	268	8	337	7	283	23	480	20
Q	49	144	7	176	5	78	10	126	7
P	60	111	6	164	7	163	19	334	23
Q	61	230	10	384	10	207	15	435	15

* Area of each count was $\frac{1}{4}$ mm^2

Area of each count was $\frac{1}{2}$ mm^2

Errors in alpha counts and Li concentrations are the 90 % confidence interval of the mean given by:

$$t_{\alpha/2} \ (S/\sqrt{n})$$

from a particular sample group (M,N,etc.) was calculated using the calibration line coefficients for that particular sample group (table A- 4). The Li concentration is given by:

$$\text{ppm Li} = (\text{counts} - a_o)/a_1$$

During the irradiation chlorite and albite from the same experiment were placed side by side. Therefore, when Li distributions were calculated errors due to any variation in neutron flux would tend to cancel. For a discussion of precision see the section on errors.

A-5 Natural chlorite and albite

The natural chlorite used consisted of two samples taken from veins in metasediments near Whitefish Falls, Ont. One of the samples was donated by D. Thompson. The chlorite coexisted with calcite and quartz. The albite used was the Ab-1 albite from Amelia County, Virginia, U.S.A.

Table A-6

measured Li in Ab-1, and chlorite

Ab-1	15	ppm ± 1
chlorite-Vilks	75	ppm ± 3
quartz found with chlorite	0	ppm ± 3
calcite found with chlorite	2	ppm ± 3

Table A-7

Analysis of chlorite using the energy dispersive

system (EDAX) on the electron microscope

SiO_2	24.99 ± 1.72	wt. %
Al_2O_3	18.44 ± 1.92	wt. %
Fe_2O_3	42.64 ± 4.66	wt. %
MgO	13.66 ± 1.86	wt. %
total	99.73	

Table A-8

X-ray diffraction study on Ab-1 and Fe-chlorites

chlorites				albites			
Vilks		Thompson		Ab-1		published values	
14.27	(25)	14.22	(23)	6.37	(7)	6.39	(20)
7.09	(90)	7.08	(93)	4.24	(2)		
4.72	(37)	4.71	(47)	4.03	(2)	4.03	(16)
3.538	(100)	3.470	(100)	3.849	(2)	3.857	(8)
2.600	(5)	2.596	(3)	3.773	(5)	3.780	(25)
2.552	(4)	2.549	(2)	3.667	(8)	3.663	(16)
2.449	(4)	2.449	(3)	3.477	(3)	3.484	(2)
2.389	(4)			3.191	(100)	3.196	(100)
2.262	(5)			2.129	(4)	2.125	(8)
1.884	(6)	1.865	(3)	2.112	(4)		
1.661	(2)			1.884	(3)	1.889	(8)
1.623	(3)			1.823	(9)		
1.565	(7)	1.565	(6)	1.802	(9)		
1.548	(2)						
1.514	(2)						

D spacings are given in angstroms.

The ralative peak heights are given as percentages by the

numbers in brackets.

A-6 Lithium concentrations in the vapor phase and lithium vapor-mineral

distributions

The Li mass balance calculations have shown that there is very poor agreement between the predicted and measured amounts of Li in the vapor phase. Since it is not clear whether the measured or the predicted Li concentrations represent the true vapor composition, both sets of data are given in table A-9. In this way the range of vapor-mineral Li distributions can be obtained because distributions calculated from predicted concentrations will be higher than those obtained from measured Li concentrations.

The averages of the distribution coefficients from table A-9 are shown in table A-10. The distribution coefficients calculated from the predicted values are higher, but in all cases the standard deviations overlap. Therefore, with the large variation in the vapor-mineral Li distributions it did not make that much difference as to which data set was used. The dependence of Li distributions on temperature was also masked by this variation.

Table A-9

Li concentration in vapor and vapor-mineral Li distributions

calculated from measured and predicted Li amounts in the vapor

| | | measured | | | predicted | | |
| | | (from col. 5, table II-4) | | | (from col. 4, table II-4) | | |
temp	sample	ppm Li in vapor	$D^{vap-alb}$	$D^{vap-chl}$	ppm Li in vapor	$D^{vap-alb}$	$D^{vap-chl}$
500	1	53	0.17	0.09	377	1.18	0.66
"	3	234	2.82	1.47	869	10.47	5.47
"	4	54	0.81	0.48	167	2.49	1.49
"	5	141	1.32	0.90	173	1.62	1.11
"	7	257	2.11	1.63	340	2.79	2.15
"	19	316	4.72	1.51	892	13.31	4.27
"	21	17	0.12	0.05	146	1.02	0.42
"	24	183	0.74	0.62	573	2.31	1.94
"	26	81	0.37	0.27	106	0.48	0.36
"	28	45	0.20	0.19	155	0.70	0.65
"	29	410	27.3	11	249	16.6	6.73
"	31	50	1.47	0.83	204	6.00	3.40
"	33	·8	0.19	0.33	244	5.81	10.17
"	38	31	0.22	0.11	31	0.22	0.11
"	39	21	0.75	0.15	155	5.54	1.14
"	40	56	1.00	0.24	86	1.54	0.38
"	41	245	4.71	2.40	209	4.02	2.05
"	42	244	7.63	2.71	256	8.00	2.48
"	43	87	2.42	0.50	157	4.36	0.91
"	47	246	4.17	1.38	632	10.71	3.55
"	48	124	0.44	0.26	118	0.42	0.25
700	35	20	0.19	0.05	144	1.38	0.38
"	37	155	3.97	0.89	341	8.74	1.95
"	60	33	0.20	0.10	808	4.96	2.42
"	61	209	1.01	0.48	570	2.75	1.31

		measured			predicted		
		(from col. 5, table II-4)			(from col. 4, table II-4)		
temp	sample	ppm Li in vapor	$D^{vap-alb}$	$D^{vap-chl}$	ppm Li in vapor	$D^{vap-alb}$	$D^{vap-chl}$
400	10	39	0.07	0.07	455	0.79	0.85
"	12	12	0.15	0.07	411	5.74	3.07
"	13	32	0.53	0.25	158	2.63	1.25
"	14	22	0.18	0.16	100	0.82	0.72
"	15	338	1.52	1.27	304	1.37	1.14
"	16	698	33	11	1030	49	16.6
"	27	156	2.84	1.30	414	7.53	3.45
"	32	86	2.87	1.32	208	6.93	3.20
600	6	14	0.04	0.02	412	1.29	0.64
"	8	91	0.30	0.14	461	1.52	0.69
"	11	9	0.26	0.20	496	14.6	11.1
"	20	4	0.05	0.04	445	5.36	4.78
"	25	13	0.37	0.17	456	13.0	5.85
"	30	117	3.16	1.63	178	4.81	2.47
"	34	7	0.10	0.05	104	1.42	0.68
"	36	8	0.10	0.03	251	3.02	0.94
"	46	219	1.96	0.96	797	7.12	3.51
"	49	6	0.08	0.05	966	12.4	7.67
		natural minerals					
500	53	94	1.49	0.64	447	7.10	3.02
"	54	128	2.84	0.95	494	11.0	3.66
"	56	72	1.33	0.49	335	6.20	2.26
"	57	89	0.48	0.62	73	0.40	0.51
"	58	39	2.44	0.37	115	7.19	1.10
"	59	802	2.37	3.34	752	2.22	3.13
"	65	539	2.12	3.64	675	2.66	4.56

Table A-10

Averaged vapor-mineral partition coefficients

group	calculated from measured Li		calculated from predicted Li	
	$D^{vap-alb}$	$D^{vap-chl}$	$D^{vap-alb}$	$D^{vap-chl}$
400^0 C	5.15 ± 11.3	1.93 ± 3.71	9.35 ± 16.3	3.79 ± 5.30
500^0 C	3.03 ± 5.91	1.29 ± 2.35	4.74 ± 4.65	2.37 ± 2.54
600^0 C	0.64 ± 1.06	0.33 ± 0.54	6.45 ± 5.13	3.83 ± 3.54
mean	2.77 ± 6.45	1.10 ± 2.31	5.97 ± 7.99	2.89 ± 3.34
with Fe-chlorite	1.87 ± 0.81	1.44 ± 1.42	5.25 ± 3.66	2.61 ± 1.42

Errors are given as standard deviations

A-7 Nature of the vapor phase in equilibrium with the minerals

This section describes the major cation composition of the solution before and after the experiment. Table A-12 gives the composition of the starting solutions and the molalities of Na, Mg, Al, and Fe (if present) in the solution removed from the capsule after the experiment. Table A-11 shows the Na, Mg, Al, and Fe analysis of international reference samples. These international reference samples were intended to be used as a comparison with the mineral analysis of experimental products and therefore less than 100 mg of each standard were analysed. The vapor samples would not encounter the same matrix interferences as the reference samples. However, the vapor analysis of Na, Mg, Al, and Fe could be subject to errors due to dilution, and possible contamination during the opening of the gold capsuls.

Table A-11

Mg, Fe, Al, and Na analysis of international reference samples

date	standard	measured	published (Abbey)	$\dfrac{measured - Abbey}{Abbey} \times 100$
		magnesium		
Aug. 7/78	granite GH	0.03 %	0.02 %	50 %
	basalt BM	6.06 %	4.50 %	35 %
		iron		
Aug. 7/78	granite GH	1.06 %	0.94 %	13 %
	basalt BM	6.51 %	6.78 %	- 4 %
		aluminum		
Aug. 7/80	granite GH	9.17 %	6.62 %	39 %
	basalt BM	10.07 %	8.57 %	18 %
		sodium		
Aug. 7/80	granite GH	2.32 %	2.86 %	- 19 %
	basalt BM	2.83 %	3.44 %	- 18 %

Four different types of solutions were used to start the experiments. The most common starting solution contained just LiCl at ppm levels (200 to 1000 ppm Li). The second and third type contained no Li. One was a 3 % NaCl brine and the other was deionized water. The fourth solution contained LiCl in a 3 % NaCl matrix. Since the solutions had been exposed to atmospheric CO_2 their pH was probably around 5.7.

When several experimental capsules were cut open their pH was immediately estimated with pH paper. The measured pH varied from 6.7 to 8. These are probably minimum values owing to contamination with the atmosphere. Volfinger (1979) reported pH values for solutions which had equilibrated with phlogopite at 600^0 C. His pH values ranged from 7.3 to 9.7. If these values represent hydrogen ion activity at high temperature then the experimental pH range may have been 7 to 9.

Using the molalities reported in table A-12 the ionic strength of the vapor was estimated. Aluminum was assumed to be present as the $Al(OH)_4^-$ complex. Helgeson (1969) showed that $Al(OH)_4^-$ dominated at pH's higher than 5 at 200^0 C. Assuming the presence of $Al(OH)_4^-$ reduces the contribution of Al on the ionic strength. Ionic strength was calculated in the usual manner.

$$I = \tfrac{1}{2} \Sigma z_s^2\, m_s$$

where: I = ionic strength

Z_s = ionic charge of s th species

m_s = molality of s th species

In order to see what vapor compositions could be expected in equilibrium with chlorite and albite, activity diagrams can be constructed with the coordinates $\log_{10}(a_{Na}/a_H)$ and $\log_{10}(a_{Mg}^2/a_H)$. Such activity diagrams in the system $Na_2O-MgO-Al_2O_3-SiO_2-H_2O$ and temperatures up to 300^0 C have been constructed by Helgeson et. al. (1969). Figure A-3 is such a diagram which has been extended to 500^0 C and pressures of 1.0 and 2.0 kb.

Table A-12

Molalities of major cations in vapor

	starting solutions		final solutions					
	ppm Li	% NaCl	m_{Na}	m_{Mg}	m_{Al}	m_{Fe}	I	I (with out Al)
			temperature	500^0 C				
1	1000	–	0.220	0.030	nd	–	–	0.17
3	500	–	0.118	0.033	nd	–	–	0.13
4	500	–	1.353	0.175	nd	–	–	1.03
5	500	–	0.338	0.812	nd	–	–	1.79
7	500	–	0.730	0.827	nd	–	–	2.02
19	1000	–	0.288	0.438	0.082	–	1.06	1.02
21	500	–	0.182	0.274	0.076	–	0.68	0.64
24	1000	–	0.315	0.430	0.109	–	1.07	1.02
26	500	–	0.264	0.055	0.029	–	0.26	0.24
28	500	–	0.187	0.064	0.020	–	0.23	0.22
29	266	–	0.218	0.391	0.082	–	0.93	0.89
31	266	–	0.444	0.201	0.066	–	0.66	0.62
33	266	–	0.268	0.097	0.034	–	0.35	0.33
38	–	–	0.180	0.066	0.045	–	0.24	0.22
39	–	–	0.188	0.076	0.025	–	0.26	0.25
40	–	–	0.203	0.076	0.038	–	0.27	0.25
41	–	3	0.698	0.103	0.044	–	0.84	0.82
42	–	3	0.662	0.189	0.066	–	1.00	0.96
43	–	3	0.531	0.041	0.023	–	0.61	0.60
47	–	3	0.694	0.295	0.117	–	1.25	1.19
48	–	3	0.143	0.069	0.046	–	0.23	0.21
			temperature	700^0 C				
35	500	–	0.185	0.255	0.031	–	0.62	0.60
37	500	–	0.751	0.282	0.035	–	0.96	0.94
60	1000	–	1.150	1.779	0.312	–	4.29	4.13
61	1000	–	1.009	0.153	0.204	–	0.91	0.81

	starting solutions		final solutions					
	ppm Li	% NaCl	m_{Na}	m_{Mg}	m_{Al}	m_{Fe}	I	I (with out Al)
			temperature	600^0 C				
6	1000	-	0.382	0.348	nd	-	-	0.89
8	1000	-	0.212	0.330	nd	-	-	0.77
11	500	-	0.198	0.110	nd	-	-	0.32
20	500	-	0.167	0.167	0.053	-	0.44	0.42
25	500	-	0.147	0.015	0.010	-	0.11	0.10
30	266	-	0.275	0.008	0.042	-	0.17	0.15
34	266	-	0.380	0.006	0.016	-	0.21	0.20
36	500	-	0.321	0.090	0.050	-	0.37	0.34
46	-	3	0.448	0.432	0.144	-	1.42	1.34
49	1000	-	0.143	0.069	0.046	-	0.23	0.21
			tempetature	400^0 C				
10	1000	-	1.330	0.532	nd	-	-	1.73
12	500	-	0.583	0.079	nd	-	-	0.45
13	250	-	0.186	0.210	nd	-	-	0.51
14	250	-	0.167	0.254	nd	-	-	0.59
15	500	-	0.226	0.385	nd	-	-	0.88
16	1000	-	0.209	0.176	nd	-	-	0.46
27	500	-	0.263	0.165	0.051	-	0.49	0.46
32	266	-	0.225	0.219	0.072	-	0.59	0.55
			natural minerals/temperature	500^0 C				
53	841	3	0.414	0.625	0.603	0.313	2.38	2.08
54	841	3	0.416	0.527	0.508	0.286	2.09	1.83
56	420	3	0.226	0.353	0.335	0.149	1.28	1.12
57	210	3	0.382	0.473	0.459	0.259	1.88	1.66
58	210	3	0.172	0.187	0.210	0.129	0.82	0.72
59	1000	-	0.360	0.211	0.231	0.162	1.04	0.93
65	841	3	0.756	0.884	0.378	0.233	2.80	2.61

nd: not determined

In the construction of figure A-3 the following phases were considered:

clinochlore	$Mg_5Al_2Si_3O_{10}(OH)_8$
kaolinite	$Al_2Si_2O_5(OH)_4$
low albite	$NaAlSi_3O_8$
Mg-montmorillonite	$Mg_{.167}Al_{2.33}Si_{3.67}O_{10}(OH)_2$
Na-montmorillonite	$Na_{.33}Al_{2.33}Si_{3.67}O_{10}(OH)_2$
pyrophyllite	$Al_2Si_4O_{10}(OH)_2$
H_2O	
$SiO_2 (aq)$	
$Mg_{(aq)}$	
$Na_{(aq)}$	

Quartz saturation controls silica activity.

The reactions shown in figure A-3 (See table A-13) were written to conserve aluminum in the solid phases. Water was added to balance oxygen. The solid phases exchange SiO_2, Mg, Na and H with the aqueous phase. Magnesium and sodium transfer is accompanied by hydrogen ion exchange. Consequently the latter three variables can be combined as a_{Mg}/a_H^2 and a_{Na}/a_H, where a_{Mg} is the activity of $Mg_{(aq)}$. Activity diagrams can be plotted with these ratios. The activity of aqueous silica must also be specified. This may be accomplished by having the system saturated with quartz or amorphous silica. The activity of H_2O and all solids is assumed to be unity.

The Gibbs free energies of all the species at 500^0 C were calculated using heat capacity coefficients given by Helgeson et. al. (1978). To calculate the change in free energies with pressure the molar volumes

Table A-13

Reactions shown in figure A-3

---

(1) $Mg_5Al_2Si_3O_{10}(OH)_8 + 3\ SiO_{2(aq)} + 2\ Na^+_{(aq)} + 8\ H^+$

(clinochlore)

$$= 2\ NaAlSi_3O_8\quad 5\ Mg^{++}_{(aq)}\quad 8\ H_2O$$

(albite)

$$\log K_1 = 5 \log (a_{Mg}/a_H^2) - 3 \log a_{SiO_{2(aq)}} - 2 \log (a_{Na}/a_H)$$

(2) $Mg_5Al_2Si_3O_{10}(OH)_8 + 0.15\ SiO_{2(aq)} + 9.72\ H^+$

(clinochlore)

$$= .858\ Mg_{.167}Al_{2.33}Si_{3.67}O_{10}(OH)_2 + 8\ H_2O + 4.86\ Mg^{++}_{(aq)}$$

(Mg-montmorillonite)

$$\log K_2 = 4.86 \log (a_{Mg}/a_H^2) - 0.15 \log a_{SiO_{2(aq)}}$$

(3) $.858\ Mg_{.167}Al_{2.33}Si_{3.67}O_{10}(OH)_2 + 2.85\ SiO_{2(aq)} + 2\ Na^+_{(aq)}$

(Mg-montmorillonite)

$$= 2\ NaAlSi_3O_8 + 0.14\ Mg^{++}_{(aq)} + 1.72\ H^+$$

(albite)

$$\log K_3 = 0.14 \log (a_{Mg}/a_H^2) - 2 \log (a_{Na}/a_H) - 2.85 \log a_{SiO_2}$$

(4) $Al_2Si_4O_{10}(OH)_2 + 2\ Na^+_{(aq)} + 2\ SiO_{2(aq)} = 2\ NaAlSi_3O_8 + 2\ H^+$

(pyrophyllite)   (albite)

$$\log K_4 = -2 \log a_{SiO_2} - 2 \log (a_{Na}/a_H)$$

(5) $.858\ Mg_{.167}Al_{2.33}Si_{3.67}O_{10}(OH)_2 + .85\ SiO_2 + .28\ H^+$

(Mg-montmorillonite)

$$= Al_2Si_4O_{10}(OH)_2 + .14\ Mg^{++}_{(aq)}$$

(pyrophyllite)

$$\log K_5 = -0.85 \log a_{SiO_{2(aq)}} + 0.14 \log (a_{Mg}/a_H^2)$$

---

of the various species were required. For minerals the molar volume at one bar and 25^0 C was used. To calculate the molar volume and the change in free energy with pressure of the aqueous species an equation of state given by Walther et. al. (1977) was used. Coefficients for this equation are given by Helgeson and Kirkham (1976).

Table A-13 summarizes the reactions which appear in figure A-3. Each curve in figure A-3 gives the activity ratios of aqueous Mg and Na in the vapor which is in equilibrium with the respective reaction. The solution compositions within the reaction boundaries are in equilibrium with the respective mineral.

Increasing pressure and decreasing temperature have the same effect on the reaction boundaries. The activity ratios tend to increase.

In order to convert the measured molalities to activities, activity coefficients were calculated. These activity coefficients, along with activity ratios are shown in table A-14. Debye-Huckel activity coefficients were calculated with the following equation:

$$\log_{10} \gamma_s = - \frac{A \; Z_s^2 \; I^{\frac{1}{2}}}{1 + a_s \; B \; I^{\frac{1}{2}}}$$

I = ionic strength

Z_s = charge of species s

a_s = ion size parameter of species s

$$A \; (T) = \frac{1.8246 \times 10^8 \cdot p_{H_2O}^{\frac{1}{2}} \; (T)}{(E \; (T) \cdot T)^{3/2}}$$

$$B(T) = \frac{50.29 \times 10^8 \cdot p_{H_2O}^{\frac{1}{2}}(T)}{(E(T) \cdot T)^{\frac{1}{2}}}$$

$p_{H_2O}(T) = $ density of water (gm/cm^3) at temperature (T)

$E(T) = $ dilectric constant of water at temperature (T)

$T = $ temperature (^0K)

At a pressure of 1.5 kb:

	400^0 C	500^0 C	600^0 C
$E(T)$	18.42	12.01	8.33
$p_{H_2O}(T)$	0.7510	0.6341	0.512
A	1.1452	1.6238	2.1048
B	0.3914×10^8	0.4156×10^8	0.4219×10^8

(1) Helgeson and Kirkham (1974 a)

(2) Kennedy and Holser (1966)

$a_{Na} = 4 \times 10^{-8}$ $\qquad\qquad$ $a_{Mg} = 8 \times 10^{-8}$

$a_{Li} = 6 \times 10^{-8}$

In figure A-3 activity ratios are plotted assuming a pH of 7 and a pH of 8. Line AB shows how the activity ratios would change with varying pH. If the pH at high temperature and pressure is still with in the range 7 to 9, the activity ratios plotted in the field of clinochlore. If the equilibrium constants and the activity coefficients are correct, the activity of Mg in the vapor is too high to be in equilibrium with the clinochlore-albite reaction as it is written. The Mg composition of the vapor seems to be controlled by clinochlore or by an incomplete clinochlore-gel reaction. To determine the effect of
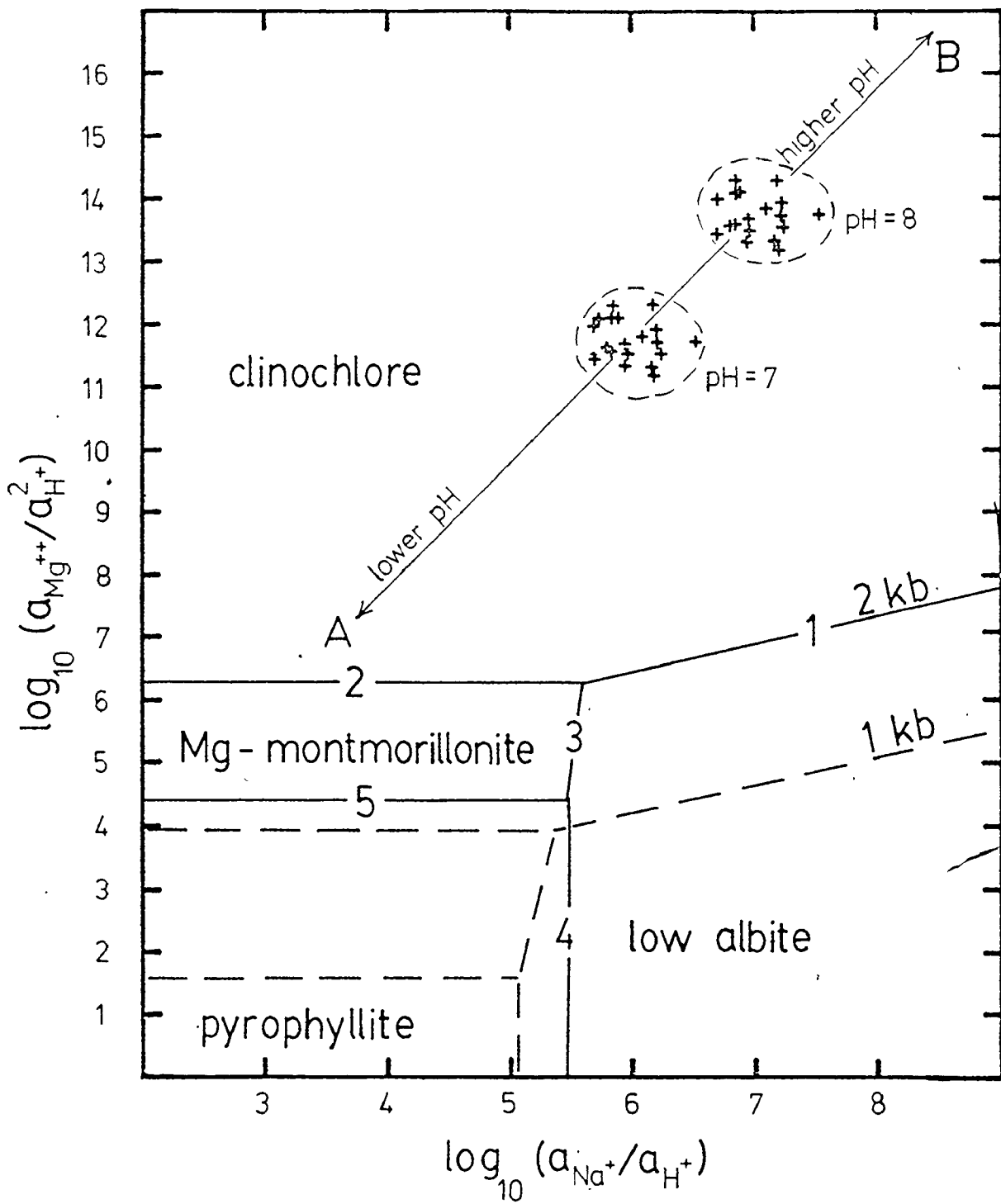
Table A-14

Activity coefficients and activity ratios

	temp	$\log\gamma_{Na}$	$\log\gamma_{Mg}$	pH = 7 $\log(m_{Na}/a_H) + \log\gamma_{Na}$	pH = 7 $\log(m_{Mg}/a_H^2) + \log\gamma_{Mg}$
1	500	-0.397	-1.130	5.95	11.35
3	"	-0.366	-1.065	5.71	11.45
4	"	-0.613	-1.507	6.52	11.74
5	"	-0.674	-1.595	5.85	12.31
7	"	-0.686	-1.612	6.18	12.31
19	"	-0.617	-1.512	5.84	12.13
21	"	-0.565	-1.431	5.70	12.01
24	"	-0.618	-1.513	5.88	12.12
26	"	-0.448	-1.229	5.97	11.51
28	"	-0.433	-1.201	5.84	11.61
29	"	-0.602	-1.489	5.74	12.10
31	"	-0.561	-1.426	6.09	11.87
33	"	-0.484	-1.296	5.95	11.70
38	"	-0.438	-1.210	5.82	11.61
39	"	-0.448	-1.229	5.82	11.65
40	"	-0.453	-1.237	5.86	11.64
41	"	-0.590	-1.471	6.25	11.56
42	"	-0.610	-1.502	6.21	11.78
43	"	-0.552	-1.410	6.18	11.20
47	"	-0.635	-1.539	6.21	11.93
48	"	-0.558	-1.420	6.16	11.34
6	600	-0.766	-1.898	5.82	11.64
8	"	-0.744	-1.865	5.58	11.65
11	"	-0.609	-1.637	5.69	11.40
20	"	-0.659	-1.724	5.56	11.50
25	"	-0.448	-1.317	5.72	10.86
30	"	-0.512	-1.451	5.93	10.45
34	"	-0.544	-1.515	6.04	10.27

	temp	$\log\gamma_{Na}$	$\log\gamma_{Mg}$	pH 7 $\log(m_{Na}/a_H) + \log\gamma_{Na}$	pH 7 $\log(m_{Mg}/a_H^2) + \log\gamma_{Mg}$
36	600	-0.632	-1.677	5.88	11.27
46	"	-0.833	-1.998	5.82	11.64
49	"	-0.558	-1.543	5.60	11.30
10	400	-0.492	-1.177	6.63	12.55
12	"	-0.375	-0.991	6.39	11.91
13	"	-0.386	-1.011	5.88	12.31
14	"	-0.399	-1.033	5.82	12.37
15	"	-0.435	-1.091	5.92	12.49
16	"	-0.377	-0.995	5.94	12.25
27	"	-0.382	-1.055	6.04	12.22
32	"	-0.399	-1.033	5.95	12.31
natural minerals					
53	500	-0.703	-1.635	5.91	12.16
54	"	-0.690	-1.617	5.93	12.10
56	")	-0.638	-1.543	5.72	12.00
57	"	-0.679	-1.602	5.90	12.07
58	"	-0.587	-1.466	5.65	11.81
59	"	-0.614	-1.509	5.94	11.82
65	"	-0.718	-1.656	6.16	12.22

Figure A-3 Activity diagram in the system $Na_2O-MgO-Al_2O_3-SiO_2-H_2O$ at 500^0 C and 1.0 and 2.0 kb. The activity ratios in a particular mineral field represent the composition of the vapor in equilibrium with that mineral. Line AB shows how the activity ratios of a solution with a given Mg/Na ratio will change with pH.

unreacted clinochlore gel, the activity ratios from the experiments
with natural minerals should be inspected (in table A-12). Experiment
65 contained a clinochlore-gel as well as iron-chlorite and albite.
The activity ratio is not significantly higher than in the experiments
which had natural chlorite. Therefore, the presence of unreacted
chlorite-gel does not explain the high Mg-activity ratios. If the
activity ratios are extrapolated to lower Mg-activities they plot in
the field of low albite. Therefore, in a vapor of this composition
albite is stable with respect to pyrophyllite and Mg-montmorillonite.

It may be argued that the high Mg-activity results from a
low temperature equilibration before the gold capsules were opened. At
1 kb. and 100^0 C the activity ratios plot close to the albite-clinochlore
reaction. However, due to the slow kinetics at low temperature and the
relatively short time involved (one day) this does not seem too likely.
Table A-15 shows averaged activity ratios at various temperatures.
There appears to be a slight increase in activity ratio with decreasing
temperature, as might be expected. A low temperature re-equilibration
would tend to mask this.

In summary, if the activity coefficients, equilibrium cons-
tants and equations are correct then the vapor composition was probably
controlled by clinochlore. Albite was stable with respect to Mg-mont-
morillonite and pyrophyllite.

Table A-15

temperature	average log (a_{Na}/a_H)		average log (a_{Mg}/a_H^2)	
400	6.07	0.29	12.30	0.19
500	5.92	0.20	12.03	0.16
600	5.76	0.17	11.15	0.51

REFERENCES

Buseck, P. R. and D. R. Veblen (1978), Trace elements, crystal defects
and high resolution electron microscopy. Geochim. Cosmochim.
Acta, 42, 669-678.

Cotton, F. A. and G. Wilkinson (1972), Advanced Inorganic Chemistry.
John Wiley and Sons.

Ellis, A. J. and W. A. J. Mahon (1964), Natural hydrothermal systems and
experimental hot-water/rock reactions. Geochim. Cosmochim.
Acta, 28, 1323-1358.

Floyd, P. A. (1977), Geochemical characteristics of upper Palaeozoic vol-
canics from S. W. England. J. Geol. Soc. London, 133, 405-406.

Fung, P. C. and D. M. Shaw (1978), Na, Rb, and Tl distribution between
phlogopite and sanidine by direct synthesis in a common
vapor phase. Geochim. Cosmochim. Acta, 42, 703-708.

Garrels, R. M. and C. L. Christ (1965), Solutions, Minerals and Equilibria,
Harper and Row.

Gordienko, V. V. and I. Y. Komentsev (1969), Effect of large cations
on structural ordering of potash feldspar. Geochemistry
International, 6, 180-192.

Heier, K. S. and G. K. Billings (1970), Lithium, in Handbook of Geochem-
istry, II/1, ed. Wedepohl, K. H., Springer-Verlag.

Helgeson, H. C. (1969), Thermodynamics of hydrothermal systems at elevated
temperatures and pressures. Am. Jour. Sci., 267, 729-804.

Helgeson, H.; T. H. Brown and T. H. Leeper (1969), Handbook of Theoretical

    Activity Diagrams Depicting Chemical Equilibria in Geological

    Systems Involving an Aqueous Phase at One Atmosphere and 0^0

    to 300^0 C. Freeman, Cooper and Company.

Helgeson, H. C. and D. H. Kirkham (1974a), Theoretical prediction of the

    thermodynamic behavior of aqueous electrolytes at high

    pressures and temperatures. (I) Summary of the thermodynamic/

    electrostatic properties of the solvent. American Journal

    of Science, 274, 1089-1198.

Helgeson, H. C. and D. H. Kirkham (1976), Theoretical prediction of the

    thermodynamic properties of aqueous electrolytes at high

    pressures and temperatures. (III) Equation of state for aqueous

    species at infinite dilution. American Journal of Science,

    276, 97-240.

Helgeson, H. C.; J. M. Delany; H. W. Nesbitt, and D. K. Bird (1978)

    Summary and critique of the thermodynamic properties of

    rock-forming minerals. American Journal of Science, 278-A.

Iiyama, J. T. (1974), Behaviour of trace elements in feldspars under

    hydrothermal conditions. In The Feldspars. Ed. W. S. MacKenzie

    and J. Zussman, Manchester Uneversity Press, 552-573.

Iiyama, J. T. (1974b), Substitution, deformation locale de la maille et

    equilibre de distribution des elements en traces entre

    silicates et solution hydrothermale. Bull. Soc. Franc. Min.

    Crist., 97, 143-151.

Iiyama, J. T. and M. Volfinger (1976), A model for trace element distribution in silicate structures. Mineral Magazine, 40, 555-564.

Kennedy, G. C. and W. T. Hoser (1966), Pressure-volume-temperature and phase relations of water and carbon dioxide. Geol. Soc. America Memoir, 97, 371-384.

Lagache, M. (1971), Etude experimentale de la repartition du cesium entre les feldspaths sodi-potassiques. Compt. Rend. Acad. Sci. Paris, 272, 1328-1330.

Liotard, J. M.; J. Vernieres; et C. Dupuy (1979), Variabilite des valeurs de coefficient de partage-influence de la structure des liquides magmatiques. Chem. Geology, 26, 237-247.

Luth, W. C. and C. O. Ingamells (1965), Gel preparation of starting materials for hydrothermal experimentation. Am. Mineralogist, 50, 255-258.

Matsui, Y.; N. Onuma; H. Nagasawa; H. Higuchi and S. Banno (1977), Crystal structural control in trace alement partition among crystals and magma. Bull. Soc. franc. Mineral. Cristallogr., 100, 315-324.

Mysen, B. O. and M. G. Seitz (1974), Trace element partitioning determined by beta track mapping: An experimental study using carbon and samarium as examples. Jour. Geophys. Res., 80, 2627-2635.

Mysen, B. O. (1978), Limits of solution of trace elements in minerals according to Henry's law: review of experimental data. Geochim. Cosmochim. Acta, 42, 871-885.

Navrotsky, A. (1978), Thermodynamics of element partitioning: (1) system-
    atics of transition metals in crystalline and molten silicates
    and (2) defect chemistry and "the Henry's Law Problem".
    Geochim. Cosmochim. Acta, 42, 887-902.

Neiva, A. M. R. (1980), Chlorite and biotite from contact metamorphism
    of phyllite and metagraywacke by granite, aplite-pegmatite
    and quartz veins. Chem. Geology, 29, 49-71.

O'Nions, R. K. and R. Powell (1977), The thermodynamics of trace element
    distribution. in Thermodynamics in Geology. Ed. D. G. Fraser,
    D. Reidel Publishing Company.

Robert, Jean-Louis et M. Volfinger (1979), Etude experimentale de
    lepidolites trioctaedriques hydroxylees. Bull. Mineral,
    102, 21-25.

Shaw, D. M.; N. Vatin-Perignon and J. R. Muysson (1977), Lithium in
    spilites. Geochim. Cosmochim. Acta, 41, 1601-1607.

Smith, J. V. (1974), Feldspar Minerals - Chemical and Textural Properties.
    2, Springer-Verlag.

Stumm, W. and J. J. Morgan (1970), Aquatic Chemistry - An Introduction
    Emphasizing Chemical Equilibrium in Natural Waters. John
    Wiley and Sons, Inc.

Thompson, G. and W. G. Melson (1972), The petrology of ocean crust across
    fracture zones in the Atlantic Oceon: evidence of a new kind
    of sea floor spreading. Jour. Geol., 80, 526-538.

Thompson, G. (1973), A geochemical study of the low temperature interaction

of seawater and oceanic igneous rock. E. O. S. Trans Am.

Geophys. Union, 54, 1015-1019.

Vine, J. D. (1976), Lithium - Nature's Lightest Metal. U. S. Department

of the Interior Geological Survey, U. S. G. S. : INF-75-27.

Volfinger, M. (1970), Partage de Na et Li entre sanidine, muscovite et

solution hydrothermale a 600^0 C et 1000 bars. C. R. Acad.

Sci., Ser. D., 271, 1345-1347.

Volfinger, M. et J. L. Robert (1979), Le lithium dans une phlogopite

de synthese. Bull. Mineral, 102, 26-32.

Walther, J. V. and H. C. Helgeson (1977), Calculation of the thermo-

dynamic properties of aqueous silica and the solubility of

quartz and its polymorphs at high pressures and temperatures.

American Journal of Science, 277, 1315-1351.

Wedepohl, K. H. (1969), Handbook of Geochemistry. Springer-Verlag.

(Supplements have been issued in 1970, 1971 and 1972 in the

form of loose-leaf volumes.)